MASSACHUSETTS INSTITUTE OF TECHNOLOGY
EXPERIMENTAL ASTRONOMY LABORATORY
Cambridge, Massachusetts 02139

PR-3

REVIEW OF NASA SPONSORED RESEARCH AT THE EXPERIMENTAL ASTRONOMY LABORATORY

January 1967

Edited by Dr. R.G. Stern

Approved: W. Markey
Director
Experimental Astronomy
Laboratory

ACKNOWLEDGMENT

This report was prepared under DSR Contract No. 76145 sponsored by the National Aeronatics and Space Administration through research grant NsG 254-62.

PR-3

REVIEW OF NASA SPONSORED RESEARCH AT THE EXPERIMENTAL ASTRONOMY LABORATORY

(Unclassified)

ABSTRACT

A review of NASA sponsored research which was held on 5 January 1967 at MIT is summarized in this report. A list of meeting attendees is included as Appendix A. Presentations were grouped into the following categories:

1. Special Topics
2. Low Level Acceleration Measurement and Related Research
3. Guidance and Control Optimization
4. Midcourse Guidance

A complete list of NASA-sponsored EAL publications is included as Appendix B.

by Robert G. Stern

January 1967

Page intentionally left blank

TABLE OF CONTENTS

TABLE OF CONTENTS (cont)

CHAPTER I

INTRODUCTION

This report contains summaries of presentations given by members of the MIT Experimental Astronomy Laboratory (EAL) in a meeting on 5 January 1967. The purpose of this meeting was to review NASA-sponsored research at EAL during the last two-year period.

The Experimental Astronomy Laboratory is one of several faculty-directed laboratories in the Department of Aeronautics and Astronautics, which is headed by Professor Raymond L. Bisplinghoff. The Laboratory is also affiliated with the MIT Center for Space Research, an interdepartmental organization directed by Professor J. V. Harrington. EAL's staff consists of four faculty members, eleven professional research engineers, and thirteen graduate research assistants. The Laboratory's founder and director is Professor Winston R. Markey.

During the past two years, more than half of the Laboratory's research has been supported by NASA under the following Grants and Contracts:

1) NsG 254-62 "Theoretical and Experimental Investigations to Determine Optimum Guidance, Navigation, and Control System and Instrumentation Concepts and Configurations for Long Term Earth-Orbiting and Interplanetary Spacecraft."

2) NGR 22-009-080 "Analytical and Experimental Investigation of Low Level Accelerometer Techniques."

3) NGR 22-009-078 "Guidance System Component Correlation Testing and Studies."

4) NAS 12-501 "Low Level Accelerometer Apparatus."

Areas in which there has been NASA-sponsered research activity at the Experimental Astronomy Laboratory during the past two years include the following:

1. Midcourse Guidance
2. Optimization

3. Statistical Filtering

4. Mission Planning

5. Navigation

6. Applied Mathematics

7. Astrophysics

8. Inertial Sensors and Test Equipment

The extent of the activity varies considerably from one area to another; currently the two areas that are receiving the greatest attention are midcourse guidance and optimization.

The midcourse guidance studies are aimed primarily at developing simple though accurate techniques for on-board computation of midcourse velocity corrections; if possible, the techniques should be simple enough to be applied manually (i. e., without the use of a digital computer). Early work at the Laboratory in this area is documented in the theses of Stern (TE-5), Gielow, Holbrow, Munnell, and Ruth, and in EAL reports by Stern (RE-4), Abrahamson and Stern (RE-14), and Tanabe (RE-20). A summary of this early work is contained in Report RE-18 by Slater and Stern. More recent theses on the same subject are those of Love, Lim, and Dierstein.

In the seminar presentations Lim (Chapter 2) has extended a study of Lambert's problem which was initiated in his master's thesis. The iterative method of solution of Lambert's problem that he has developed is simple enough to be computed manually and has good convergence properties. It is applicable to all types of conic sections.

Curry (Chapter 3) has extended the analysis made by Slater and Stern in RE-18. Whereas the earlier work compared various simplified guidance methods for a prescribed set of initial conditions, Curry has considered a statistical distribution of initial conditions in making his comparisons.

All of the work completed to date has made use of adaptations of two-body models to develop simplified guidance techniques. In contrast, Carlson (Chapter 4) is using a basic three-body model. By applying the method of matched asymptotic expansions, he is attempting to develop an analytic solution to the guidance problem which is more accurate than any of the two-body solutions and yet is simple enough so that the required computations can be performed manually.

Statistical filtering and optimization may be regarded as two facets of a single general problem. "Filtering" is normally associated with the estimation

of the state of a dynamical system for which redundant, but noisy, measurements are available; "optimization" is usually associated with the control of a dynamical system. The two can be considered individually, or they can be combined in the development of an optimum strategy.

Early work at EAL in statistical filtering consists of a report by Potter and Stern (RE-3) and two additional reports by Potter (RE-9 and RE-11). Optimization of the control of deterministic systems is treated by Stern and Potter (RE-17) and in theses by Winston and Eck.

Current work at EAL in these areas was reported by five of the seminar speakers. Fagan (Chapter 5) has optimized the scheduling of on-board navigational measurements by use of the method of steepest descent. The results indicate an interesting clustering of measurements at discrete measurement times.

Prussing (Chapter 6) is using a relatively simple mathematical model to obtain an analytic (rather than purely numerical) solution to the problem of optimal multiple-impulse orbital rendevous. The analysis is restricted to consideration of circular trajectories. Results indicate that, depending on initial conditions, either two, three, or four impulses are optimal.

Deyst (Chapter 7) has developed an optimal guidance strategy for a class of systems for which the available measurements are noisy. Numerical solution of the problem is accomplished by the use of dynamic programming. The procedure is of practical interest when the number of control variables is relatively small (e.g., one or two).

Rockwell (Chapter 8) has developed an efficient computational algorithm for optimizing the determination of a set of unconstrained control parameters in a nonlinear system such that some specified quadratic form in the related state parameters is minimized. There is an interesting geometric interpretation of the method.

Price (Chapter 9) has applied the principles of optimal control to the problem of a soft landing on the moon. The cost function that he is minimizing includes a measure of trajectory smoothness and time during which the astronaut can view the landing site, as well as fuel consumed. The problem treated is a time-open problem; i.e., in addition to the components of the thrust control vector, final time is also considered in the optimization procedure.

EAL activity in mission planning was initiated by the thesis of Hollister (TE-4) and continued in a study by Hollister and Prussing (RE-16) of powered

flybys of Venus on a trip from Earth to Mars. Young (Chapter 10) has written a computer program which seeks out opportune times for flybys of both Venus and Mars on round trips which start and end at Earth. The program was carried out by making use of the time-sharing facilities at the M. I. T. Computation Center; it is a good illustration of the effective use of these facilities.

In the area of navigation, a simplified approach to the problem of selecting optical sightings for position determination in interplanetary space was given by Stern (RE-7). The determination of the optimum times for optical sightings was investigated in a thesis by Fagan and Whitlow and extended in the work reported by Fagan in Chapter 5.

McDonald (Chapter 11) has initiated a new phase in EAL's navigation studies. He has investigated the feasibility of using a gyrocompass as an attitude reference for a spacecraft. A more complete report of this study is RE-21.

McDonald has also supervised two theses relating to navigation problems of Sunblazer, a small unmanned solar probe. These were written by Madl (CSR T-66-4) and by Doerer and Langley (CSR T-66-5).

Current work in applied mathematics at EAL is under the direction of Madden, who recently joined the staff. In Chapter 12 he reports on a method of estimation of a function when a finite number of its moments is known. The method yields definitive upper and lower error bounds.

A mathematical technique that currently is being applied to a variety of problems is the method of matched asymptotic expansions. In Chapter 13 Willes has applied the method to the problem of atmospheric entry. This work is soon to be published as a doctoral thesis. Carlson in Chapter 4 has applied the method to the three-body problem.

Research in astrophysics has recently been initiated at EAL. This work has been undertaken jointly with Lincoln Laboratory. Dr. I. I. Shapiro, of Lincoln Laboratory, is directing the effort. Counselman (Chapter 14) has been investigating mathematical models which might explain the recently observed axial rotation of the planet Mercury.

Three of the seminar presentations involve hardware development. In Chapter 15, Ezekiel has described the low-level acceleration measurement apparatus development initiated at EAL and now being carried on at the NASA Electronic Research Center in Cambridge. This work is described in greater detail in RE-23. A second presentation by Ezekiel, in Chapter 16, discusses a technique for long-term stabilization of laser frequency. Finally, Egan, in

Chapter 17, describes the development of a test table for the evaluation of the performance of high-accuracy accelerometers and gyros.

Of the fifteen people making technical presentations at the seminar, nine are M. I. T. graduate students who are currently working on their doctoral theses.

CHAPTER II

A NEW SOLUTION TO LAMBERT'S PROBLEM

by

Wai K. Lim

Lambert's theorem states that the time t to traverse a conic arc depends only upon the length of the major axis, a, the sum $(r_1 + r_2)$ of the distances of the initial and final points of the arc from the center of force, and the length, d, of the chord joining these points. For orbit determination purposes, one has to solve for the semi-major axis given $r_1 + r_2$, d, and t. Considering the transcendental nature of the flight time equations, a solution can be obtained only by some kind of iterative method. The convergence and simplicity of the iterative solution depends on the form of the equation and the variable iterated. This report[1] presents a new form of the flight time equation in terms of a variable, q, which is related to the mean of the two eccentric anomalies.

The new method of solving Lambert's problem has certain advantages and disadvantages when compared with the classical method[2] and the uniform variable method[3]. In the classical method, the semi-major axis, a, is used to determine the conic section. While this parameter has the advantage of providing a uniform representation of all solutions, it suffers from two defects. First, the series representation of the solution involves the inverse sine function which requires more terms in the series than the sine function for the same numerical accuracy. Second, the flight time is related to the parameter in a complicated manner requiring careful knowledge of multiple solution.

The uniform variable method uses the regularized eccentric anomaly, Φ^2, which is defined as the square of the difference of the two eccentric anomalies. It is a uniform solution in the sense that the resulting flight time formula is valid for elliptic, parabolic, and hyperbolic orbits. There are two disadvantages in this method. First, the representation of the solution involves at least two series which have to be evaluated specifically for this purpose. Second, for multiperiod transfer, Φ^2 is large and the convergence of the series requires increasing numbers of terms to be computed.

In the present method, the series representation of the solution involves only the sine function (or hyperbolic sine in the case of hyperbolic transfer). Because the magnitude of the independent variable, q, is confined to the interval $[0, \pi]$, the series can be truncated after the first few terms. Another advantage

of this form of flight time equation is the simplicity of the equation when time is normalized with respect to the physical quantity $\sqrt{\frac{(r_1 + r_2)^3}{2\mu}}$ and the geometry of the problem is represented by a single parameter, $\sqrt{1 - \left(\frac{d}{\gamma_1 + \gamma_2}\right)^2}$. The disadvantage of this method when compared with the method of Uniform Variable is that three different formulas have to be used rather than one.

A test program was written for the IBM7094 computer. With the same input data, it solved Lambert's problem using each of the three methods in sequence. By averaging the time interval between the beginning and end of each iteration for one thousand iterations, the computation time per iteration was found for each of the three methods tested. The result (see Fig. 5) showed that the present method is at least twice as fast as the other two. The computation times quoted here do not include input/output time or the time spent in setting up the output format. Consequently, they indicate the relative number of algebraic operations performed in a single iteration which are required by each of the methods. A number of test cases are used to determine the accuracy in orbit determination (in terms of orbital velocity computed) obtainable using a single-precision program and the number of iterations it takes to reach a solution. The conclusion (see Fig. 6) is that the classical method converges more slowly and is less accurate. In both respects, convergence and accuracy, the uniform variable method and the present method are comparable.

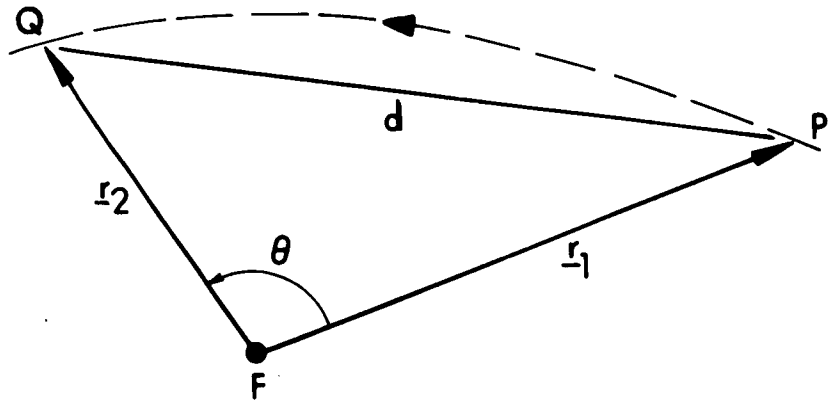

Fig. 1 Geometry of Lambert's Problem.

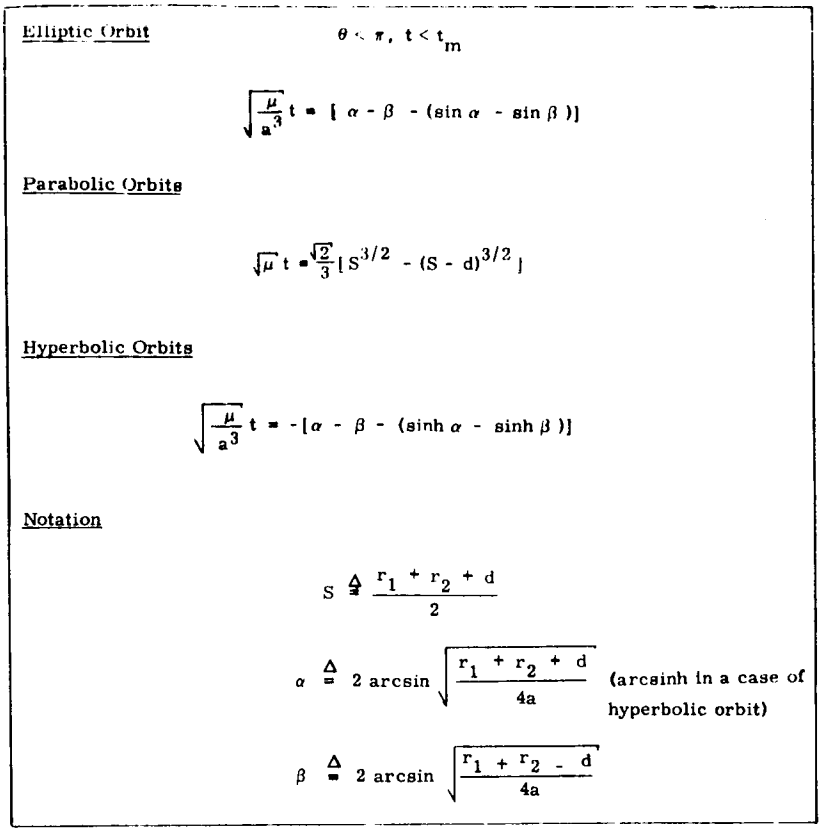

Fig. 2 Classical time of flight equations.

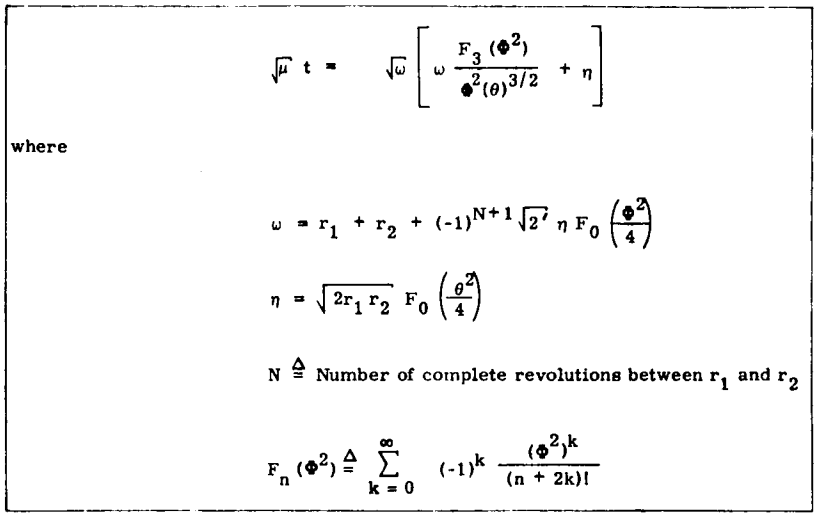

Fig. 3 Time of flight equation in terms of uniform variable.

Elliptic Orbit

$$\sqrt{\frac{2\mu}{(r_1 + r_2)^3}}\, t = \sqrt{\frac{1 - W\cos q}{\sin^3 q}}\, [(N\pi + q) - \sin q \cos q + W(\sin q - (N\pi + q)\cos q)]$$

Parabolic Orbit

$$\sqrt{\frac{2\mu}{(r_1 + r_2)^3}}\, t = \frac{1}{3}(2 + W)\sqrt{1 - W}$$

Hyperbolic Orbit

$$\sqrt{\frac{2\mu}{(r_1 + r_2)^3}}\, t = -\sqrt{\frac{1 - W\cosh q}{\sinh^3 q}}\, [q - \sinh q \cosh q + W(\sinh q - q\cosh q)]$$

$$-\text{Arc}\cosh\left(\frac{1}{W}\right) < q < 0$$

$$W \triangleq \sqrt{1 - \left(\frac{d}{r_1 + r_2}\right)^2}$$

Fig. 4 New time of flight equation.

Method	Computation Time per Iteration (10^{-3} seconds in IBM 7094)
Classic	7.4
Uniform Variable	5.8
Present Method	2.8

Fig. 5 Comparison I.

Test Case	V m/sec	Classic N	Classic ΔV	Uniform Variable N	Uniform Variable ΔV	Present Method N	Present Method ΔV
Hyperbolic							
2[a] Near Parabolic	43,000			8	1.1×10^{-3}	6	5.6×10^{-4}
1[a] Typical	45,000			5	2.3×10^{0}	8	1.1×10^{-3}
Elliptic							
1. Typical	33,000	6	1.6×10^{-2}	8	2.8×10^{-4}	6	1.1×10^{-3}
2 Near Parabolic	42,000	15	3.8×10^{-2}	4	5.6×10^{-4}	7	8.5×10^{-3}

N = Number of iterations before a convergence solution is obtained

ΔV = Increment of V at N^{th} iteration

V = Orbital velocity

Fig. 6 Comparison II.

REFERENCES

1 Lim, W.K., "Explicit Non-linear Two-body Guidance Analysis", S.M. Thesis, January, 1966, M.I.T. Dept. of Aeronautics and Astronautics.

2 Battin, R.H., Astronautical Guidance, Mc Graw Hill, 1964.

3 Pines, S., "A Uniform Solution of Lambert's Problem", NASA MSC Internal Note No. 65-FM-166, December 1965.

CHAPTER III

STATISTICAL EVALUATION OF SIMPLIFIED MIDCOURSE GUIDANCE LAWS

by

R. E. Curry

I. INTRODUCTION

Previous investigations of simplified guidance techniques[1, 2, 3] have dealt with the problem of examining relative accuracies for a specific sampling of launch errors. This procedure is straightforward and is as follows:

GIVEN:
1. No Uncertainties
2. Nominal Trajectory
3. Correction Times
4. Launch Error
5. Guidance Law

TEST PROCEDURE

1. Integrate from launch state to find target error.
2. Use guidance law (at first correction) to attempt to null target error.
3. Integrate results of guidance correction to find residual target error.
4. Repeat steps 2 and 3 for each maneuver point.

The purpose of this analysis is to obtain a quantitative measure of guidance law accuracies based on launch error statistics rather than a specific sampling of the launch errors. One such measure of accuracy is the RMS target error due to guidance law computation.

The approach taken here is to linearize nonlinear guidance laws so that the velocity correction becomes a linear combination of the vehicle's state. The second order statistics of the target error then become a function of the guidance law and launch error statistics.

II. ANALYSIS

The following assumptions are made for this analysis:

ASSUMPTIONS

1. Impulsive Thrusting
2. Linearized Equations of Motion
3. Linear Guidance Laws

Result: Many-Body-Linear Guidance Law is exact (to first order).

Equations of Motion

As a result of the above assumptions the following linear difference equations describe the state deviations from nominal:

$$\delta x_i^- = \Phi_{i,\, i-1}\, \delta x_{i-1}^+ \quad (\delta x_0 = \text{Launch Error})$$

$$\delta x_i^+ = b_i + \psi_i\, \delta x_i^-$$

$$(\delta x_D)i = \Phi_{D,\, i}\, \delta x_i^+$$

where

δx_i^- = state deviation at i^{th} correction time before correction

δx_i^+ = state deviation at i^{th} correction time after correction

$\Phi_{i,\, i-1}$ = transition matrix of linearized deviations from nominal between $(i-1)^{st}$ and i^{th} correction

$\Phi_{D,\, i}$ = transition matrix from i^{th} correction to destination

b_i = bias in i^{th} correction

ψ_i = guidance matrix at i^{th} correction

$(\delta x_D)i$ = target error after i^{th} correction.

The second moment matrices of the above random vectors may easily be found recursively using the covariance matrix of launch errors as an initial condition.

Linearization of Guidance Laws

The following non linear guidance laws are being examined:

GUIDANCE LAWS

1. Implicit Position Offset
2. Implicit Velocity Offset
3. Explicit Position Offset
4. Explicit Velocity Offset

The word "implicit" is used here to denote guidance schemes that use a precomputed reference trajectory; "explicit" techniques do not use a precomputed reference trajectory.

All four guidance laws are non linear and use a conic trajectory approximation

which accounts for perturbation accelerations, but neglects the gradient of the perturbation accelerations with respect to position. See Reference 1 for details.

It has been found necessary in this study to make the distinction between the "nominal" and "reference" trajectories. A nominal trajectory is that which would be followed if no launch errors or other errors were present. The implicit guidance techniques considered here use the nominal trajectory as a reference.

The explicit guidance schemes use a reference trajectory computed at each maneuver point by integrating the full equations of motion forward from a prescribed set of initial conditions. Two obvious choices of initial conditions are

EXPLICIT REFERENCE TRAJECTORIES

Integrate equations of motion from
TYPE A: Present position and velocity
TYPE B: Present position and velocity of Lambert conic to target

It has been found from experience that for reasonable injection errors the Type A reference trajectory usually misses the target by much more than the Type B reference. On the other hand, the Type A reference may be used in an iterative manner if the position and velocity of the last iteration are used in place of the "present" position and velocity. These characteristics suggest the following iteration scheme: use the Type B reference for the first reference trajectory and the Type A reference for all subsequent iterations.

Only the Type B reference trajectories have been considered for the following reasons:

1. Only non iterative solutions to the guidance problem are being considered.
2. The Type B trajectories are usually closer to the target, and linearization about them will be more accurate.

III CONCLUSION TO DATE

1. Linearized Implicit Guidance Laws differ only in the reference conic used.
2. Linearized Explicit (Type B reference) Guidance Laws
   a. Reduce to same guidance law
   b. Contain velocity correction bias error

The linearized implicit guidance laws use the two-body transition matrix of a reference conic: the implicit position offset method linearizes about the osculating conic at the nominal correction time; the implicit velocity offset method linearizes about the nominal Lambert conic at the correction time. (The nominal Lambert conic is defined by the position on the nominal trajectory at the correction time

and by the target position at the final time.)

The linearized explicit guidance schemes yield the same velocity correction for the Type B reference. In addition, there is a velocity correction bias error inherent with the Type B reference trajectory. This bias error indicates that a maneuver should be made even if the nominal trajectory is being followed. The basic cause of such behavior is the neglect of the gradient of the perturbing accelerations and the choice of reference trajectory.

IV. FUTURE WORK

Future work in this area will consist of numerical evaluation of RMS target errors for the above mentioned guidance laws. Another facet which merits investigation is the statistical behavior of the error in an iterative solution to an explicit guidance problem.

REFERENCES

1 Slater, G. L., Stern, R. G., "Simplified Midcourse Guidance Techniques", AIAA/AAS Stepping Stones to Mars, Baltimore, Md., March 1966.

2 Munnell, T. C., "An Analysis of the Application of Two-Body Linear Guidance to Space Flight", S. M. Thesis in Department of Aeronautics and Astronautics, MIT, August 1964.

3 Gielow, R. L., "An Evaluation of the Two-Body Non-Linear Interplanetary Guidance Technique", S. M. Thesis in Department of Aeronautics and Astronautics, MIT, May 1964.

CHAPTER IV

MANUAL ON-BOARD GUIDANCE FOR MANY-BODY INTERPLANETARY TRAJECTORIES

by

N.A. Carlson

Introduction

Navigation and guidance for unmanned lunar and interplanetary space missions are currently performed by means of Earth-based radar tracking, digital computation, and radio command signals. For manned missions, on-board navigation and guidance represent an alternative which is attractive not only near the target, where radio transmission time from the Earth can be significant, but also as a back-up system for use in case of communications failure.

On-board guidance requires a digital computer to perform numerical integration and matrix manipulation, but should entail a manual mode as well because of the possibility of computer breakdown during the extended flight times of interplanetary missions. Manual guidance must circumvent the numerical integration capability of the computer with analytic solutions for interplanetary trajectories, perhaps in conjunction with tabular data, these being sufficiently accurate for guidance purposes.

Previous Work

Simplified on-board guidance techniques generally have made use of the analytic behavior of two-body trajectories to reduce the requirements for digital computation [1,2,3]. Implicit techniques utilize stored data from a precomputed reference trajectory to eliminate on-board numerical integration, and explicit techniques require no reference but presently rely on numerical integration and the analytic properties of Keplerian orbits. The capability for major post-launch mission changes and abort trajectories evidently favors explicit techniques. Furthermore, the high sensitivity of the near-target trajectory to midcourse variations limits the validity of linearization about a pre-planned reference.

An explicit manual guidance scheme requires analytic solutions for many-body trajectories passing close to the target planet. The many-body problem, in particular planetary perturbation theory, [4,5,6] has been studied for over two hundred years. Perturbation solutions in terms of power series expansions have been obtained, but generally under the implicit assumption that the body of interest

never passes close to a perturbing planet. As a first approximation to many-body spacecraft trajectories, the patched-conic model has been widely used in mission planning, but is crude for guidance purposes[2]. The method of matched asymptotic expansions has more recently been applied to lunar[7] and interplanetary[8,9] trajectory analysis to include perturbations ignored in the patched-conic model. Though the matching of perturbed conics has been effected in terms of bounded definite integrals, analytic perturbation solutions still are not available. These solutions or the equivalent are essential to the explicit manual guidance formulation.

Current Investigation

To determine approximate perturbation solutions uniformly valid over the midcourse and terminal portions of the trajectory, the author is applying the method of matched asymptotic expansions in a fashion similar to that of Perko[8,9] and Breakwell[9]. The three-body problem is examined first, the three bodies specified for convenience to be the Sun, Mars, and the spacecraft (see Fig. 1).

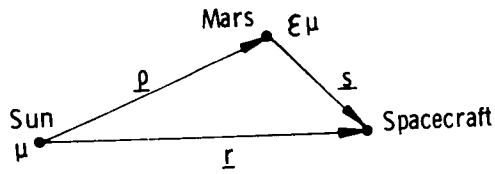

Fig. 1 Three-body problem.

The equations of spacecraft motion relative to the Sun and to Mars and that of Mars relative to the Sun are respectively,

$$\ddot{\underline{r}} = -\frac{\mu}{r^3}\underline{r} - \epsilon\mu\left[\frac{\underline{s}}{s^3} + \frac{\underline{\rho}}{\rho^3}\right] \tag{1}$$

$$\ddot{\underline{s}} = -\frac{\epsilon\mu}{s^3}\underline{s} - \mu\left[\frac{\underline{r}}{r^3} - \frac{\underline{\rho}}{\rho^3}\right] \tag{2}$$

$$\ddot{\underline{\rho}} = -(1+\epsilon)\frac{\mu}{\rho^3}\underline{\rho} \tag{3}$$

Note that the Martian orbit is Keplerian in this context, and that the solution of either Eq (1) or Eq (2), given the Martian orbit, is sufficient to define the spacecraft trajectory.

The "outer" or heliocentric perturbation solution is obtained by expanding $\underline{r}$ in a power series in the small parameter ϵ

$$\underline{r} = \underline{r}_0 + \epsilon\underline{r}_1 + \epsilon^2\underline{r}_2 + \ldots \tag{4}$$

Substituting this expression into the Taylor expansion of Eq (1) and equating coefficients of equal powers of ϵ yields

$$\ddot{\underline{r}}_0 = -\frac{\mu}{r_0^3}\underline{r}_0 \tag{5}$$

$$\ddot{\underline{r}}_1 = G(\underline{r}_0)\underline{r}_1 - \mu\left[\frac{\underline{r}_0 - \underline{\rho}}{|\underline{r}_0 - \underline{\rho}|^3} + \frac{\underline{\rho}}{\rho^3}\right] \tag{6}$$

$$\ddot{\underline{r}}_2 = G(\underline{r}_0)\underline{r}_2 + \frac{1}{2}\underline{r}_1^T H(\underline{r}_0)\underline{r}_1 + G(\underline{r}_0 - \underline{\rho})\underline{r}_1 \tag{7}$$

and so on, where G is the gravity gradient matrix and H represents the second gradient, a third order tensor. $\underline{r}_0$ is a Keplerian ellipse, and $\underline{r}_1$ and $\underline{r}_2$ can be written in terms of the linearized state transition matrix evaluated on this ellipse, e.g.,

$$\underline{r}_1(t) = M(t,t_0)\underline{r}_1(t_0) + N(t,t_0)\dot{\underline{r}}_1(t_0) - \mu\int_{t_0}^{t} N(t,\tau)\left[\frac{\underline{r}_0 - \underline{\rho}}{|\underline{r}_0 - \underline{\rho}|^3} + \frac{\underline{\rho}}{\rho^3}\right]_\tau d\tau \tag{8}$$

$$\underline{r}_2(t) = M(t,t_0)\underline{r}_2(t_0) + N(t,t_0)\dot{\underline{r}}_2(t_0) + \int_{t_0}^{t} N(t,\tau)\left[\frac{1}{2}\underline{r}_1^T H(\underline{r}_0)\underline{r}_1 + G(\underline{r}_0 - \underline{\rho})\underline{r}_1\right]_\tau d\tau \tag{9}$$

where

$$M(t,t_0) = \frac{\partial \underline{r}_0(t)}{\partial \underline{r}_0(t_0)}, \quad N(t,t_0) = \frac{\partial \underline{r}_0(t)}{\partial \dot{\underline{r}}_0(t_0)} \tag{10}$$

Though the perturbation integrals involve known implicit functions of time, they cannot be integrated analytically in a straightforward manner. However, the asymptotic behavior of the integrals as $\underline{r}_0$ approaches $\underline{\rho}$ can be determined by taking Taylor expansions in time relative to the zero-order intercept time[8]. The resulting asymptotic solution can be matched with the asymptotic "inner" or planetocentric solution, but involves certain bounded definite integrals that cannot be evaluated analytically.

The inner solution is most easily examined by defining the "stretched" inner variables

$$\tau = \frac{t}{\epsilon}, \quad \underline{\sigma} = \frac{\underline{s}}{\epsilon} \tag{11}$$

Using these variables in Eq (2) and expanding the solar perturbation term under the assumption that $s << \rho$ yield

$$\underline{\sigma}'' = -\frac{\mu}{\sigma^3}\,\underline{\sigma} + \epsilon\, G(\rho)\,\epsilon\,\underline{\sigma} + \ldots \tag{12}$$

Writing $\underline{\sigma}$ as a power series in ϵ and proceeding as before result in the following equations:

$$\underline{\sigma}_0'' = -\frac{\mu}{\sigma_0^3}\,\underline{\sigma}_0 \tag{13}$$

$$\underline{\sigma}_1'' = G(\underline{\sigma}_0)\,\underline{\sigma}_1 \tag{14}$$

$$\underline{\sigma}_2'' = G(\underline{\sigma}_0)\,\underline{\sigma}_2 + \frac{1}{2}\,\underline{\sigma}_1^{T} H(\underline{\sigma}_0)\,\underline{\sigma}_1 + G(\rho)\,\underline{\sigma}_0 \tag{15}$$

and so on. The inner solution is Keplerian and can be obtained analytically through first order in the region $\frac{s}{\rho} \leq 0(\epsilon)$.

It should be noted that different solution regions can be defined by employing different stretching factors to balance different terms in the equations of motion. For example, stretching both the time and distance variables by $\epsilon^{1/2}$

$$\tau = \frac{t}{\epsilon^{1/2}}\,, \quad \underline{\varsigma} = \frac{\underline{s}}{\epsilon^{1/2}} \tag{16}$$

and expanding $\underline{\sigma}$ in terms of $\epsilon^{1/2}$, assuming $\frac{s}{\rho} \leq 0(\epsilon^{1/2})$, result in

$$\underline{\sigma}_0'' = \underline{0} \tag{17}$$

$$\underline{\sigma}_{1/2}'' = -\frac{\mu}{\sigma_0^3}\,\underline{\sigma}_0 \tag{18}$$

$$\underline{\sigma}_1'' = G(\underline{\sigma}_0)\,\underline{\sigma}_{1/2} + G(\rho)\,\underline{\sigma}_0 \tag{19}$$

and so on. Here the zero-order solution is straight-line motion; the half- and first-order solutions can be obtained analytically. The region defined by Eq (16) thus yields directly the asymptotic planetocentric trajectory, and may presumably be matched with the inner solution defined by Eqs (13) - (15) on the one side and the outer solution defined by Eqs (5) - (7) on the other.

The basic unsolved problem thus seems to be the determination of an analytic solution to the perturbed heliocentric motion defined by Eqs (6) and (7), in particular to evaluating the associated perturbation integrals:

$$\Delta \underline{r}_1(t) = -\mu \int_{t_0}^{t} N(t,\tau) \left[\frac{\underline{r}_0 - \underline{\rho}}{\left| \underline{r}_0 - \underline{\rho} \right|^3} + \frac{\underline{\rho}}{\rho^3} \right]_\tau d\tau \qquad (20)$$

$$\Delta \underline{r}_2(t) = \int_{t_0}^{t} N(t,\tau) \left[\frac{1}{2} \underline{r}_1^T H(\underline{r}_0) \underline{r}_1 + G(\underline{r}_0 - \underline{\rho}) \underline{r}_1 \right]_\tau d\tau \qquad (21)$$

Future Work

Integration of the first-order perturbation integral (20) is obviously of primary concern. The integration can in fact be carried out under various simplifying assumptions, for example that $(\underline{r}_0 - \underline{\rho})$ is a linear vector function of time and that $N(t,\tau)$ can be represented by a truncated Taylor series in time. In addition, the classical perturbation theory for planetary motion can be applied when the spacecraft is not close to the planet. Evaluation of the second-order perturbation integral (21) will involve similar simplifications should it prove significant for guidance purposes, as will evaluation of the perturbation integrals due to non-target planets, such as Jupiter.

In light of the current status of the investigation, future work shall proceed according to the following plan:

1. Evaluate the significant perturbation integrals by various simplifying approximations, including planetary theory.
2. Investigate the use of tabular data in conjunction with partial analytic solutions to the perturbation integrals.
3. Match the resulting inner and outer solutions asymptotically to determine a uniformly valid solution.
4. Formulate guidance equations, including the possible use of tabular data.
5. Evaluate the accuracy of candidate guidance formulations by comparison with numerical results and by possible application of Perko's error analysis[8].
6. Determine the time required for manual computation of a guidance correction by each of the candidate formulations.
7. Compare guidance accuracy with the expected accuracy of on-board navigation and implementation of guidance corrections; define a practical limit to required guidance accuracy and associated computation.

REFERENCES

1 Slater, G. L., and R. G. Stern, "Simplified Midcourse Guidance Techniques", M.I.T. Experimental Astronomy Laboratory Report RE-18, February 1966.

2 Munnell, T. C., "An Analysis of the Application of Two-Body Linear Guidance to Space Flight", S. M. Thesis, Department of Aeronautics and Astronautics, M.I.T., August 1964.

3 Battin, R. H., "Explicit and Unified Methods of Spacecraft Guidance Applied to Lunar Missions", paper presented at XVth International Astronautical Congress, Warsaw, Poland, September 1964.

4 Smart, W. M., Celestial Mechanics, Longmans, Green and Co., New York, 1953.

5 Brown, E. W., and C. A. Shook, Planetary Theory, Dover Publications, Inc., New York, 1964.

6 Dziobek, Otto, Mathematical Theories of Planetary Motions, Dover Publications, Inc., New York, 1962.

7 Lagerstrom, P. A., and J. Kevorkian, "Earth-to-Moon Trajectories in the Restricted Three-Body Problem", Journal de Méchanique, June 1963.

8 Perko, L. M., "Asymptotic Matching in the Restricted Three-Body Problem", Ph. D. Thesis, Department of Mathematics, Stanford University, December 1964.

9 Breakwell, J. V., and L. M. Perko, "Matched Asymptotic Expansions, Patched Conics, and the Computation of Interplanetary Trajectories", AIAA Paper 65-689, September 1965.

CHAPTER V

OPTIMUM NAVIGATION MEASUREMENTS

by

John H. Fagan

The scheduling for sightings for use in a self-contained space navigation system represents a trade-off between the accuracy of navigation and the cost of making the sightings. This cost includes the attitude control fuel required to re-orient the spacecraft, fuel required for stabilization, and the time that astronauts are diverted from other tasks to make the sightings.

Previous attempts at schedule optimization include the determination of the best sightings at pre-selected times and the effect of alternate navigation schemes on guidance fuel requirements. In a more recent study, a steepest descents approach was applied to determine, for the reduction of in-plane position uncertainties in a circular earth orbit, the optimum times for making star-horizon sightings. Results indicated that a grouping of sightings about certain optimum times, rather than a continuous distribution, resulted in more accurate position estimates for the same number of measurements. This paper is a continuation of the above work in which it is sought to establish a general framework for the determination of navigation schedules which minimize estimation uncertainty for a fixed number of measurements or, equivalently, obtain a given uncertainty with the minimum number of measurements.

The extension of the problem includes consideration of out-of-plane errors and schedule optimization not only for the sighting times, but for the best sightings as well. From the preliminary study, it is assumed that there will be some grouping of sightings at the same time. As a first simplification, the time required to make the sightings is considered negligible with respect to the mission time. Also, an unlimited field of eligible stars is assumed available. A reasonably general cost function is selected which weights navigational uncertainty at times t_k, when velocity corrections are made, and at the end of the mission, t_p. Expressed in terms of E, the covariance matrix of estimation errors, the total uncertainty,

$$U = \sum_{k=1}^{P} \mathrm{tr}\,(Q_k E_k) \qquad (1)$$

where the Q matrices determine the weightings.

Assuming that the navigation schedule will consist of N groups, each containing n_k statistically identical sightings, the processed information, S, can be expressed as follows:

$$E^{-1} = S = \sum_{k=1}^{N} n_k J_k \tag{2}$$

where J_k is the information contained in one sighting. A completely optimum schedule is determined by the variation of three parameters: the sighting time, t_k; the the number of sightings at each time, n_k; and the sighting information matrix, J_k. The problem is further simplified by considering only star-horizon sightings, for which Eq (2) becomes:

$$E^{-1} = S = \sum_{K=1}^{N} n_k \frac{\Phi_{Nk}^{-T} \underline{h}_k \underline{h}_k^T \Phi_{Nk}^{-1}}{\sigma_k^2} \tag{3}$$

$\underline{h}_k$ is the geometry vector (as shown in slides #1 and #2), σ_k^2 is the variance of the sighting noise and Φ_{Nk}, the state transition matrix by which information is referred to a later time. For star-horizon sightings, the locus of possible orientations of $\underline{h}$ at any given time is a cone whose elements are perpendicular to the line of sight to the planet edge.

Because the collected information is linear in n_k, a steepest descent approach to the variational problem results in a simple, analytical set of influence coefficients.

Influence coefficients for the remaining two variables, t_k and $\underline{h}_k$, are not so easily obtained because of the complex functions involved. However, by some manipulation, all three sets of coefficients can be interrelated so that a reasonably simple steepest descent optimization procedure is established. A two-body environment is assumed for the example problems and possible correlations between errors in successive sightings are neglected. For simplicity, the terminal point uncertainty in position and velocity is considered. The velocity elements are scaled by 100 min^2 for dimensional compatibility. From Eq (1)

$$U = \text{tr}\left[\begin{Bmatrix} I_3 & O_3 \\ O_3 & \tau^2 I_3 \end{Bmatrix} E_p\right] \qquad \tau = 10 \text{ min} \tag{4}$$

Two trajectories are investigated; a circular satellite orbit and a hyperbolic free-fall re-entry. The state estimation in both cases is obtained by thirty-two star horizon sightings, accurate to one minute of arc.

The combined effect of the assumption of two-body motion and the selection of a diagonal weighting matrix produces an inherent decoupling of the in- and out-of-plane error propagation in the problems considered. Given these conditions, it is established that an arrangement of sightings which preserves this decoupling always results in a better estimate. Therefore, instead of a unique sighting direction at each optimum sighting time, four different configurations are possible, (as shown in slides #1 and #2).

The computer solutions (pictured in slides #3 and #4) both exhibit the grouping phenomenon encountered in the preliminary study. A concentration of sighting at the boundaries of a trajectory seems to be characteristic of this type of problem. The particular time locations of sightings and their distribution along the trajectory is a strong function of the cost considered. For example, terminal position information is generally best obtained by measurements near the end of the trajectory, whereas the best velocity estimates derive from evenly distributed measurements.

The component rms estimate uncertainties resulting from the computer optimization are compared (slide #5) to those obtained from more conventional schedules in which the sightings are evenly distributed along the trajectory. The numerical improvements are intended only as an indication of the effectiveness of grouped sightings. In addition to the enhanced estimation accuracy, there is an inherent fuel saving in this navigation scheme, since the spacecraft need only be positioned for sightings a few times throughtout the mission. It is this grouping phenomenon that emerges as the significant result of the study. The symmetric arrangement of the sightings is a special case resulting from simplifying assumptions. As long as the system cost function can be expressed as in (1), an upper limit on the number of optimum times can be defined. In fact, for cost functions of this general type, both necessary and sufficient conditions can be defined, establishing the computer solution as a true optimum.

At present, the same basic optimization procedure is being applied to an orbit determination problem by Angus Morrison of EAL. It is felt that a representative cost function can be established in the form of Eq (1). If so, the solution obtained should contain a limited number of sighting locations and should also be established as a true optimum solution. If Morrison's work does turn out this way, it will provide a strong corroboration of the grouped measurement scheme since traditional methods of orbit determination employ many evenly spaced sightings. The basic contention is that any problem which can be formulated in this manner should show the same results.

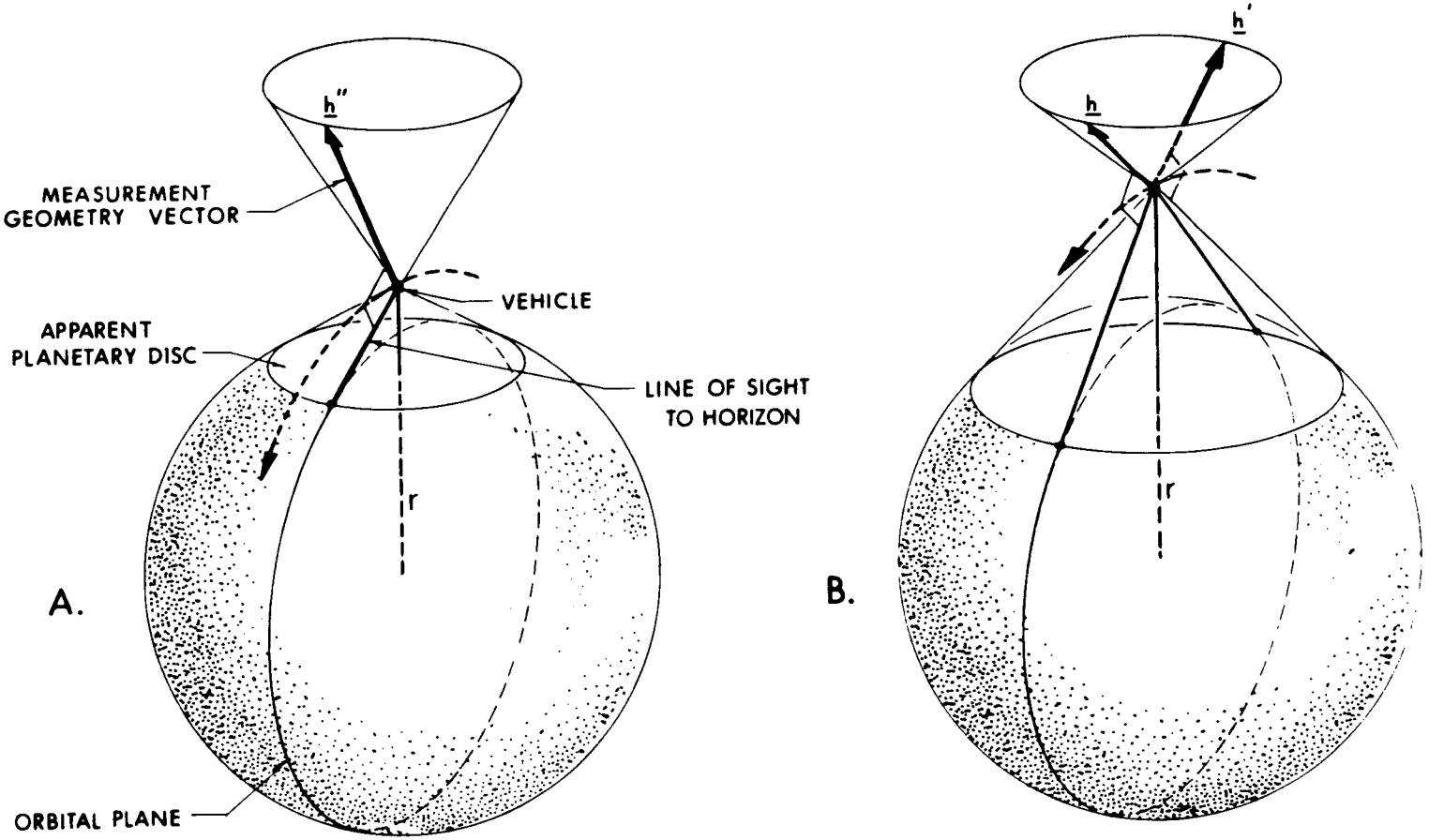

Fig. 1 Possible sighting configurations A and B.

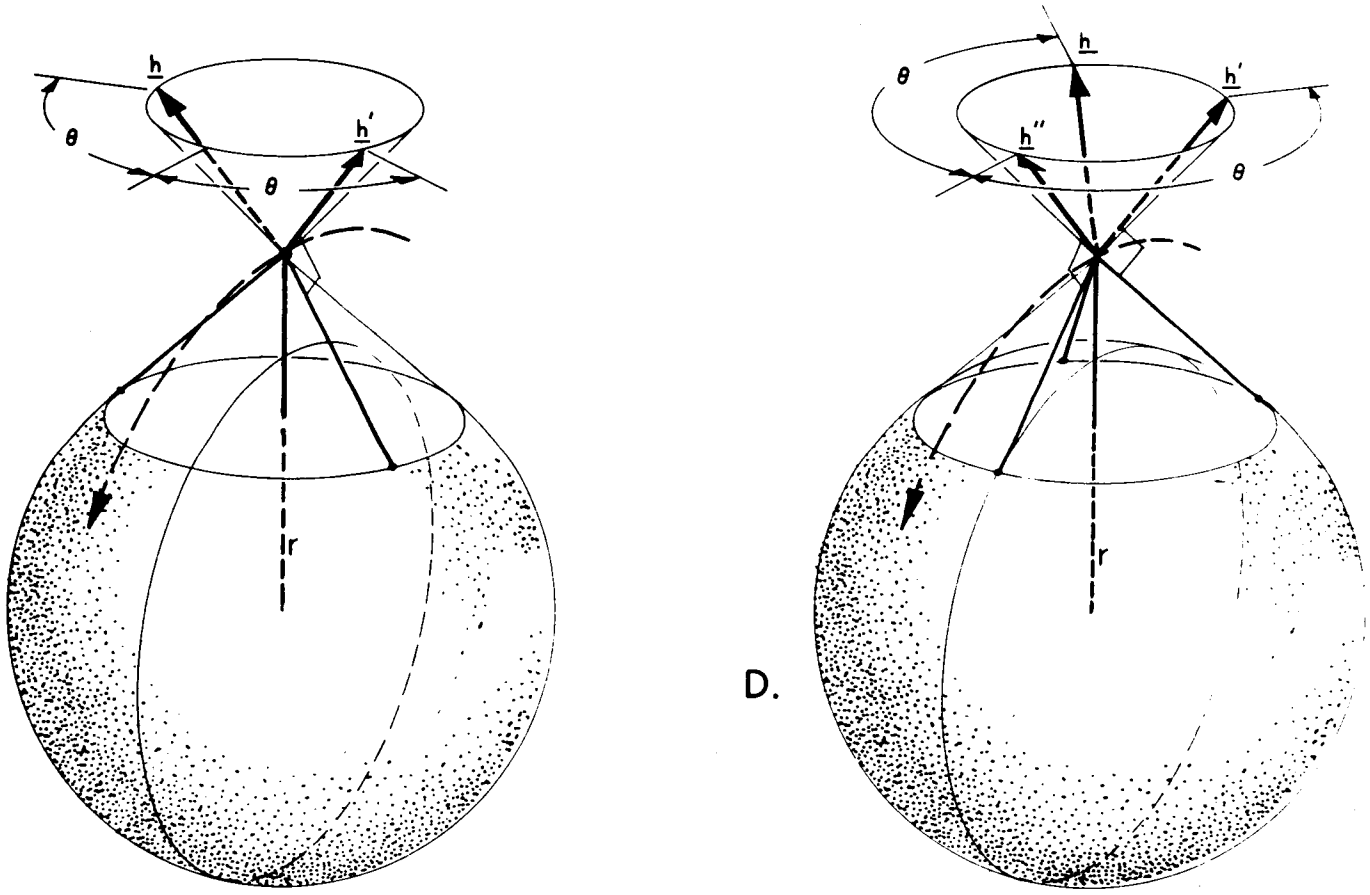

Fig. 2 Possible sighting configurations C and D.

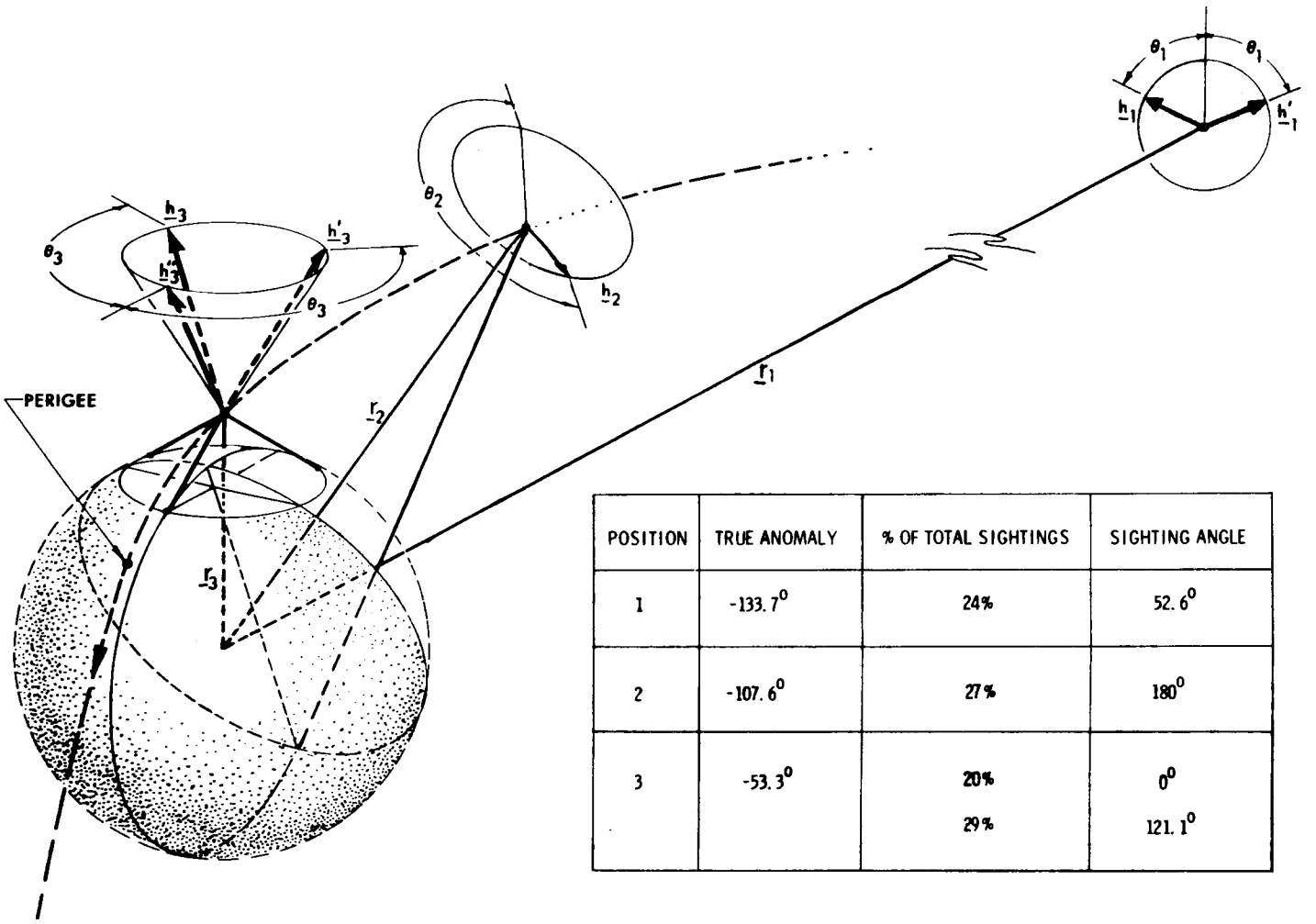

POSITION	TRUE ANOMALY	% OF TOTAL SIGHTINGS	SIGHTING ANGLE
1	-133.7^0	24%	52.6^0
2	-107.6^0	27%	180^0
3	-53.3^0	20% 29%	0^0 121.1^0

Fig. 3 Optimum solution - hyperbolic trajectory.

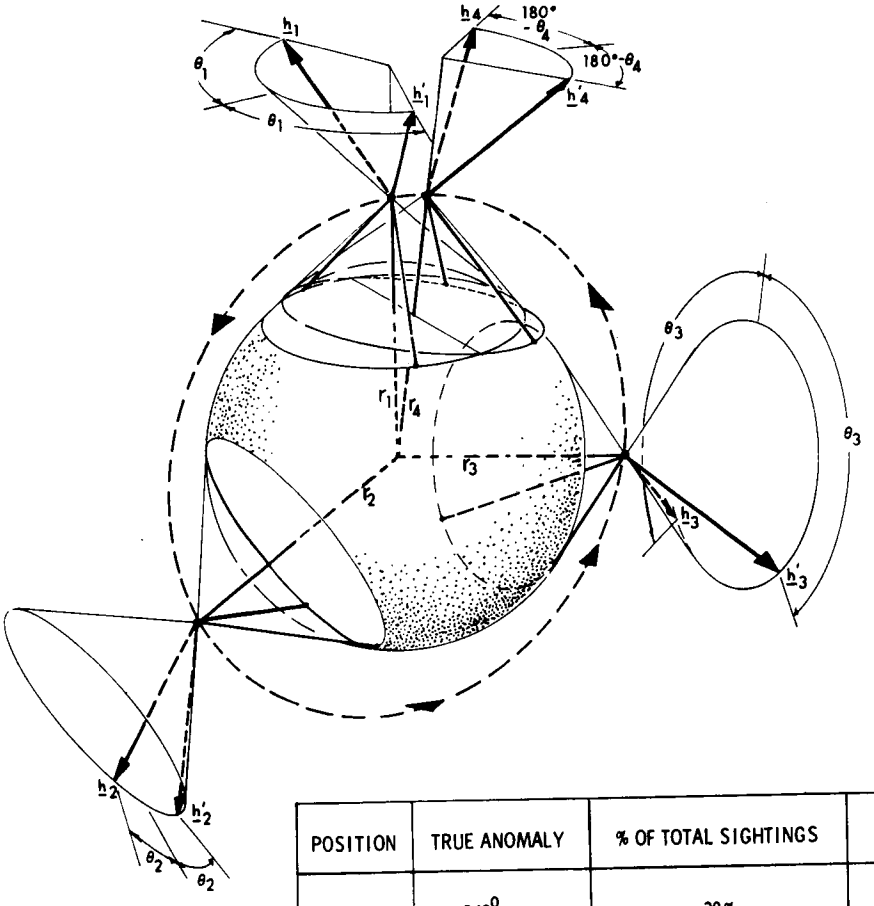

POSITION	TRUE ANOMALY	% OF TOTAL SIGHTINGS	SIGHTING ANGLE
1	-360^0	39%	70.1^0
2	-241.9^0	7%	13.7^0
3	-93.7^0	13%	147.6^0
4	-6.4^0	41%	160.8^0

Fig. 4 Optimum solution - circular orbit.

HYPERBOLIC TRAJECTORY

	r_r	r_s	r_z	v_r	v_s	v_z
OPTIMUM	1240	1158	950	1.95	1.02	1.47
Δt SPACING	16620	46100	28420	34.61	9.88	47.60
Δf SPACING	5750	13620	9625	9.19	2.58	11.51

CIRCULAR ORBIT

	r_r	r_s	r_z	v_r	v_s	v_z
OPTIMUM	1698	2015	2020	0.43	0.30	1.15
Δt SPACING	3348	4180	4150	0.87	0.61	2.00

Fig. 5 Comparison of position and velocity rms uncertainty. Units: meters, meters/sec in target rsz coordinates.

CHAPTER VI

OPTIMAL MULTIPLE-IMPULSE ORBITAL RENDEZVOUS

by

John Prussing

ABSTRACT

Minimum fuel orbital transfer in an inverse square force field has been a subject of considerable interest. One aspect of this problem is Lawden's problem, the minimum fuel transfer of a variable-thrust rocket having constant exhaust velocity and unbounded thrust magnitude. Reference 1 gives a concise summary of the known solutions to Lawden's problem. Many solutions to Lawden's problem are known for the time-open case, in which the transfer time is not fixed. One well-known solution of this type is the Hohmann transfer. For the time-fixed case not many results have been obtained. This is the subject of the present investigation.

A rendezvous between two orbits in a fixed time can always be accomplished with two impulses. However, in some situations, this may require excessive fuel. One example of this is a 180° non-nodal transfer between inclined orbits. In this case a third, mid-course impulse can reduce the fuel consumption considerably. The existence of three-impulse solutions which are superior to two-impulse transfers in some situations and the likelihood that more than three impulses is superior for some transfers warrants the present investigation of multiple impulse transfers.

The method used is an application of the theoretical work of Lawden[2], in which the necessary conditions for a minimizing transfer are described in terms of the primer vector, the adjoint to the first order variation in velocity. The three conditions which must be satisfied for an optimal impulsive transfer are:

(1) The thrusts are to be applied at the times for which the primer has unit magnitude.

(2) At these times the thrust direction is to be aligned with the primer.

(3) The magnitude of the primer must not exceed unity during the transfer.

Figure 1 shows the behavior of the magnitude of the primer vector for an optimal three-impulse transfer.

From a solution for the primer vector which satisfies the conditions for an optimal transfer, one obtains the times of application and the directions of the thrust impulses. The magnitudes of the impulses must then be determined by solving the boundary value problem for the rendezvous.

If one considers rendezvous between two low-eccentricity orbits which lie close to one another, a linear boundary value problem may be formulated by linearizing the equations of motion about an intermediate reference orbit.

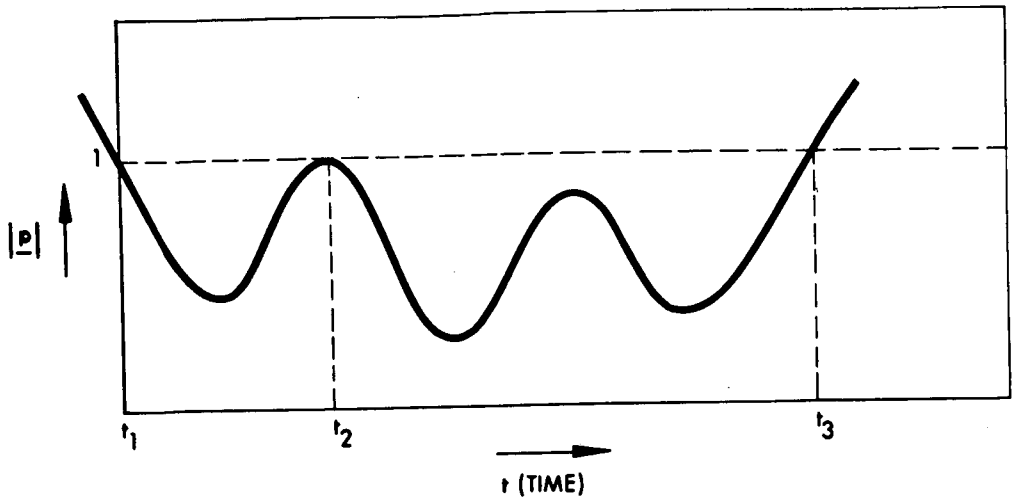

Fig. 1 Primer Vector Magnitude for optimal 3-impulse transfer.

Let $\delta \underline{x}(t_F)$ be the desired state variation (the state variation of the target) at the final time. Considering the state vector to have q components, an n-impulse rendezvous can be described as

$$\delta \underline{x}(t_F) = \Phi(t_F, t_0)\, \delta \underline{x}(t_0) + W \Delta \underline{v}$$

where $\Phi(t_F, t_0)$ is the q x q state transition matrix between the initial and final time.

$\Delta \underline{v}$ is an n component vector having as components the magnitudes of the velocity changes caused by the thrust impulses.

W is a q×n matrix of weighting coefficients which are functions of the optimal times of correction, t_j, and the unit vectors in the directions of thrust, $\underline{u}_j$. For an n-impulse rendezvous W has n columns. Each column is of the form:

$$\underline{w}_j = \frac{\partial \underline{x}(t_F)}{\partial \underline{v}(t_j)} \underline{u}_j$$

The solution of the boundary value problem is the determination of the $\Delta \underline{v}$ which will rendezvous with the target in the specified time. This boundary value solution is obtained analytically.

If the reference orbit is circular, the expression for the primer vector along the reference and the variational equations of motion have a relatively simple form. In order to get an analytical solution which will simply describe how many impulses are optimal for different rendezvous situations, this investigation assumes that both the reference orbit and the initial and final orbits are circular and coplanar.

For a linear problem it is known that the minimum fuel transfer can be accomplished with a number of impulses equal to at most the number of specified state variables in the final orbit.[3] [4] For a coplanar rendezvous, the maximum number of impulses necessary for an optimal transfer is four.

The solutions to the circle-to-circle, coplanar rendezvous which have been obtained to-date are:

(1) Four-impulse rendezvous transfers.

(2) Three-impulse rendezvous transfers having an initial or final coasting period.

(3) Hohmann rendezvous transfers having an initial and/or final coasting period.

In solutions (2) and (3) a coasting period is allowed which does not exist for the four-impulse case. Since the transfer time is fixed, impulses may not always occur at the terminals of the transfer and coasting periods may be required.

As an example, a three-impulse primer solution may be used to obtain an optimal two-impulse transfer with an initial coasting period. This is shown in Fig. 2. In this application the fixed transfer time is $t_3 - t_0$. As seen in the figure, the first impulse does not occur until t_2; therefore $t_2 - t_0$ is the coasting period in the initial orbit which will result in an optimal transfer for the specified transfer time.

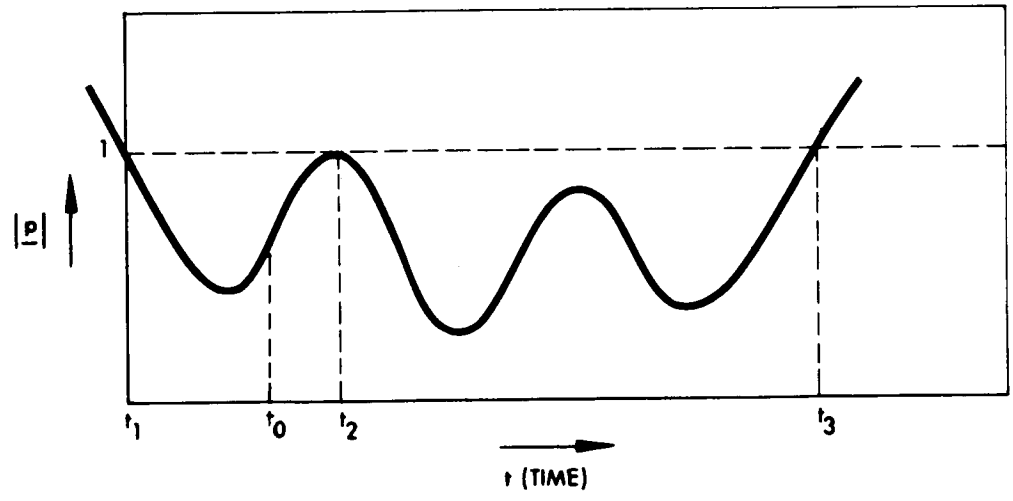

Fig. 2 Primer magnitude for optimal 2-impulse transfer with initial coast.

Fig. 3 shows four-impulse solutions for a special case of the circle-to-circle problem. In this case the initial and final orbits are the same orbit; the problem is then to transfer to another point in the orbit in a specified amount of time. The two-impulse solution, which has a singularity near 500^{o}, is also shown for comparison. Note that the range

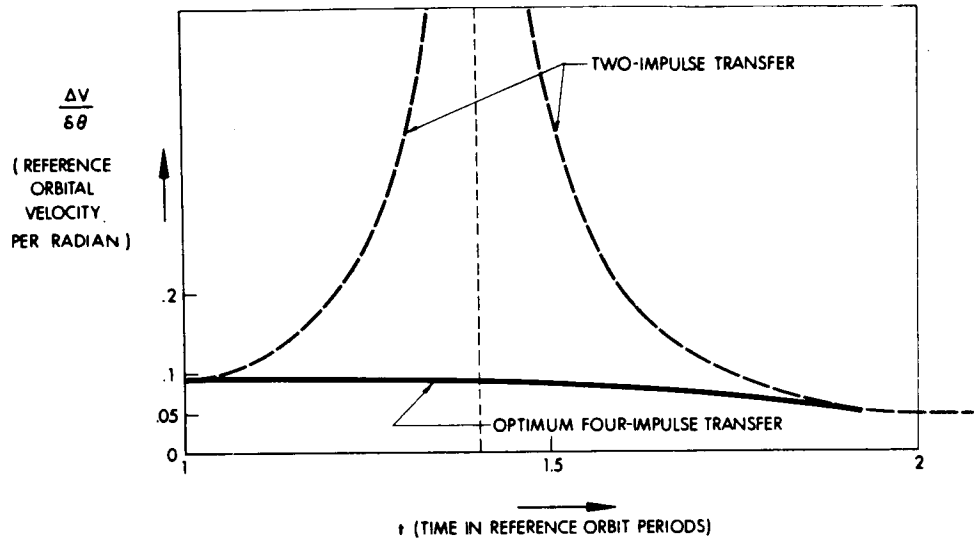

Fig. 3 Circle-to-circle, coplanar transfers ($\delta R \equiv 0$).

of transfer times for optimal circle-to-circle four-impulse transfers is greater than one reference orbit period.

Figure 4 shows the three types of solutions obtained to-date. For this figure the reference orbit is chosen to be half-way between the initial and final orbits.

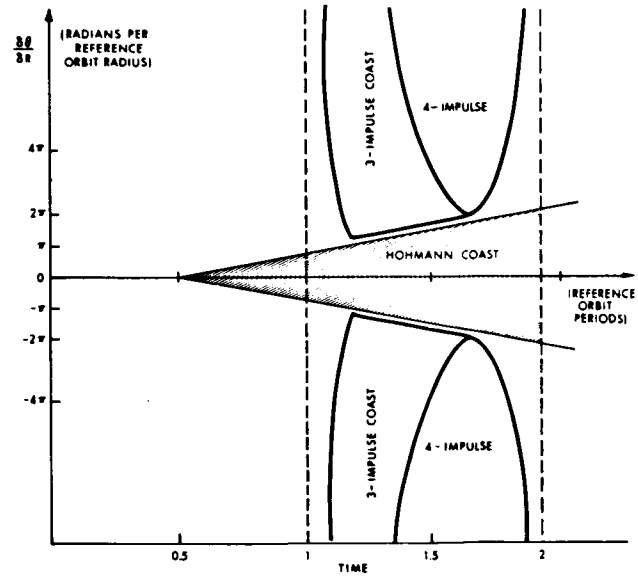

Fig. 4 Partial Plot of Reachable States Using Optimum Transfers (Circle-to-circle, coplanar).

The minimum transfer time boundary for both the four-impulse and the three-impulse with coast is the same.

The solutions which remain to be investigated are other three-impulse solutions and the optimal two-impulse solutions.

REFERENCES

1 Edelbaum, T. N., "How Many Impulses?", AIAA Paper No. 66-7, AIAA Third Aerospace Sciences Meeting, New York, January 1966.

2 Lawden, D. F., Optimal Trajectories for Space Navigation, Butterworths, London, 1963.

3 Neustadt, L. W., "Optimization, A Moment Problem and Nonlinear Programming", SIAM J. on Control 2, 1964.

4 Potter, J. E. and R. G. Stern, "Optimization of Midcourse Velocity Corrections", IFAC Symposium on Automatic Control in the Peaceful Uses of Space, Stavanger, Norway, June 1965.

CHAPTER VII

OPTIMAL CONTROL IN THE PRESENCE OF MEASUREMENT UNCERTAINTIES

by

John Deyst

This research is concerned with the problem of optimal control of linear stochastic systems when the information available to the controller contains random disturbances. In particular we wish to solve problems for which the cost may be a non-quadratic function of the state variables and/or the control variables. We assume that the system may be described by discrete equations; however, the theory may be generalized to include continuous problems.

For discrete problems we wish to consider the following equations

$$x(n+1) = \Phi(n+1, n)\, x(n) + \theta(n+1, n)\, u(n) + v(n) \tag{1}$$

$$\begin{aligned} &E[v(n)] = 0 \\ &E[v(n)\, v^T(n)] = V(n) \\ &E[v(n)\, v^T(i)] = 0 \qquad i \neq n \end{aligned} \tag{2}$$

$$m(n) = H(n)\, x(n) + w(n) \tag{3}$$

$$\begin{aligned} &E[w(n)] = 0 \\ &E[w(n)\, w^T(n)] = W(n) \\ &E[w(n)\, w^T(i)] = 0 \qquad i \neq n \end{aligned} \tag{4}$$

$$J = E\left[\sum_{n=1}^{q} L(x(n), u(n), n) + \phi(x(q+1))\right] \tag{5}$$

$x(n)$ is the system state vector at time t_n, Φ is the state transition matrix, u is a control vector, θ is the control sensitivity matrix, and v is normally distributed process disturbance with statistics as shown. The initial state, $x(0)$, is a vector of normally distributed random variables with known statistics. The controller has available to it the measurement process, $m(n)$. $H(n)$ is the measurement matrix and $w(n)$ is a normally distributed measurement error with statistics as shown. The controller may use the entire past history of measurements $\{m(0), m(1), \ldots, m(n)\}$ to determine the control to be applied at t_n. We wish to determine the control as a function of these measurements so as to minimize the expected cost J. It is important to note that the incremental cost, L, and the terminal cost, ϕ, are not required to be quadratic in x or u.

Now consider the following equations:

$$\hat{x}'(n+1) = \Phi(n+1, n)\,\hat{x}(n) + \theta(n+1, n)\,u(n) \tag{6}$$

$$\hat{x}(n) = \hat{x}'(n) + P'(n)\,H^T(n)\left[H(n)\,P'(n)\,H^T(n) + W(n)\right]^{-1} \times \left[m(n) - H(n)\,\hat{x}'(n)\right] \tag{7}$$

$$P'(n+1) = \Phi(n+1, n)\,P(n)\,\Phi^T(n+1, n) + V(n) \tag{8}$$

$$P(n) = P'(n) - P'(n)\,H^T(n)\left[H(n)\,P'(n)\,H^T(n) + W(n)\right]^{-1} H(n)\,P'(n) \tag{9}$$

$$x(n) = \hat{x}(n) - e(n) \tag{10}$$

$$f_{x(n)}(\xi \mid \hat{x}(n)) = (2\pi)^{-k/2}\,|P(n)|^{-1/2} \exp\left\{-1/2\left[\xi - \hat{x}(n)\right]^T \times P(n)^{-1}\left[\xi - \hat{x}(n)\right]\right\} \tag{11}$$

Equations (6) - (9) are the Kalman estimation equations, generalized to include the effect of the control $u(n)$. $P(n)$ is the covariance matrix of estimation errors. If $e(n)$ is the estimation error then the state at time t_n can be written as Eq (10). Now $e(n)$ is normally distributed with mean zero and covariance $P(n)$. Also, it can be shown that $e(n)$ is independent of $\hat{x}(n)$. It follows that posterior probability density for $x(n)$, given the measurement history up to time t_n, is given by (11). Equation (11) represents a normally distributed random variable with posterior mean $\hat{x}(n)$ and covariance $P(n)$. We assume that $P(n)$ is known a priori so that $\hat{x}(n)$ determines the posterior probability density for $x(n)$. Thus $\hat{x}(n)$ is a sufficient statistic because it embodies all knowledge of $x(n)$ obtained from the measurement history.

Let us now consider a vector $s(n)$ defined by Eq (12). $s(n)$ is the incremental change in the estimated state, $\hat{x}(n)$, as a result of processing the measurement $m(n)$. Thus $\hat{x}(n)$ may be written as in Eq (13). It can be shown that $s(n)$ is normally distributed with statistics given by Eq (14) and its probability density appears as Eq (15).

$$s(n) = P'(n)\,H^T(n)\left[H(n)\,P'(n)\,H^T(n) + W(n)\right]^{-1}\left[m(n) - H(n)\,\hat{x}'(n)\right] \tag{12}$$

$$\hat{x}(n) = \Phi(n, n-1)\,\hat{x}(n-1) + \theta(n, n-1)\,u(n-1) + s(n) \tag{13}$$

$$E\left[s(n)\right] = 0$$

$$E\left[s(n)\, s^T(n)\right] = S(n) = P'(n)\, H^T(n) \left[H(n)\, P'(n)\, H^T(n) + W(n)\right]^{-1} \times H(n)\, P'(n) \tag{14}$$

$$E\left[s(n)\, s^T(i)\right] = 0 \qquad i \neq n$$

$$f_{s(n)}(\zeta) = (2\pi)^{-k/2} \left|S(n)\right|^{-1/2} \exp\left\{-1/2 \zeta^T\ S(n)^{-1}\ \zeta\right\} \tag{15}$$

The last of Eqs (14) is quite important because it indicates that the s(n) are independent increments.

Let us now define a minimum expected value function, C*, as the minimum expected cost to complete the process from some arbitrary time, t_n, given the measurement history up to time t_n. Since C* is a conditional expectation, depending upon the measurement history, it is a deterministic function of the past measurements. It can be shown however that C* may be written as a function of the sufficient statistic $\hat{x}(n)$ and that C* must satisfy the recursion formula (16).

$$C^*(\hat{x}(n), n) = \min_{u(n)} \left\{ L^*(\hat{x}(n), u(n), n) + \int_{-\infty}^{\infty} d\zeta_1 \cdots \int_{-\infty}^{\infty} d\zeta_k\, f_{s(n+1)}(\zeta)\, C^* \times (\hat{x}'(n+1) + \zeta, n+1) \right\} \tag{16}$$

$$L^*(\hat{x}(n), u(n), n) = \int_{-\infty}^{\infty} d\xi_1 \cdots \int_{-\infty}^{\infty} d\xi_k\, f_{x(n)}(\xi \mid \hat{x}(n))\, L(\xi, u(n), n) \tag{17}$$

$$\hat{x}'(n+1) = \Phi(n+1, n)\, \hat{x}(n) + \theta(n+1, n)\, u(n) \tag{18}$$

$$C^*(\hat{x}(q+1), q+1) = \phi^*(\hat{x}(q+1)) \qquad t_{q+1} = \text{final time} \tag{19}$$

$$\phi^*(\hat{x}(q+1)) = \int_{-\infty}^{\infty} d\xi_1 \cdots \int_{-\infty}^{\infty} d\xi_k\, f_{x(q+1)}(\xi \mid \hat{x}(q+1))\, \phi(\xi) \tag{20}$$

The function L* in (16) is the expected incremental cost at time t_n, given the measurement history. Since C* is a function of $\hat{x}(n)$, the minimization required on the right of (16) produces the optimal control as a function of the estimate $\hat{x}(n)$. Also $f_{x(n)}(\xi \mid \hat{x}(n))$ and $f_{s(n)}(\zeta)$ are known a priori, so the set of equations (16) - (20) is complete and the optimal control as a function of $\hat{x}(n)$ can be obtained a priori by their solution.

The following diagram illustrates the optimal control system:

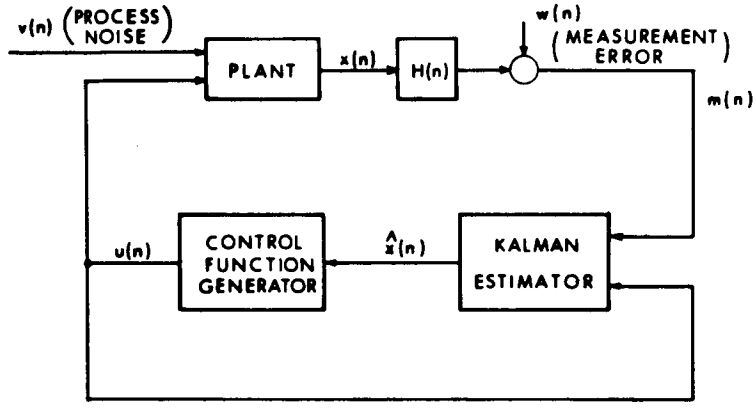

For most practical problems, solution of (16)-(20) requires digital computation. A useful property of the density functions appearing in (16), (17), and (20) is that they are the Green's functions for a multidimensional diffusion equations. Therefore, instead of performing multidimensional integrations, it may be computationally advantageous to approximate the solution of the diffusion equations by central differences.

The theory outlined above has been applied to the problem of minimum mean fuel for midcourse guidance corrections of spacecraft. If the out-of-plane errors are ignored, the midcourse guidance problem has four state variables, two for position and two for velocity. Measurements are made using ground-based radar and estimates of spacecraft position and velocity are calculated. Two velocity corrections are made. The second is a total correction which completely nulls the estimated miss distance at the target. The first correction is calculated to minimize the total mean fuel required to make both corrections. The following diagram illustrates the Earth-to-Mars spacecraft trajectory which serves as the reference.

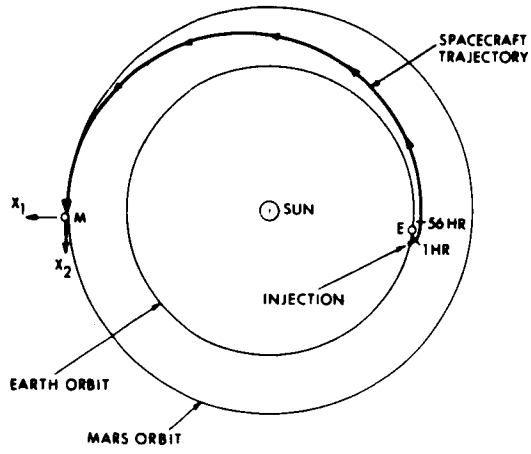

And the optimal control at the first correction time is determined from the following diagram:

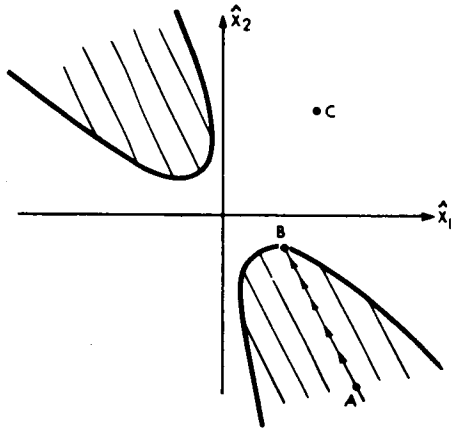

Coordinate $\hat{x}_2$ is the estimated target miss distance at the target, in the direction of the reference trajectory. $\hat{x}_1$ is the estimated target miss distance at the target, in the direction perpendicular to the reference trajectory. If the estimated miss before a velocity correction occurs at point A, then the optimal impulsive velocity correction drives the estimated state to point B. If, however, the estimated target miss is at point C, no correction is applied at the first correction time. Thus the optimal control at the first correction time is either zero, or of magnitude such that it drives the estimated state to the threshold. This of course is typical of all minimum fuel solutions including the deterministic cases.

Finally, it should be clearly understood that the numerical solution of these problems becomes extemely difficult as the number of state variables increases. Essentially, the solutions require Dynamic Programming with all the concomitant numerical difficulties. There are, however, a number of useful applications of the theory to problems of small dimensionality.

CHAPTER VIII

LINEAR PARAMETER OPTIMIZATION WITH QUADRATIC COST: A SUMMARY

by
Donald Rockwell

Problem Statement and Summary

The problem considered is that of choosing a set of unconstrained parameters, (u), so as to minimize a positive, definite, quadratic form in x(u):

$$J(u) = x(u)^T A x(u)$$

Here x is an nxl "state" vector that depends numerically on u, the mxl "control" vector ($m \leq n$). The problem is solved approximately by assuming x to be nearly linear in u near the optimum point u^o. With this assumption, J is closely approximated by the function:

$$J(u) = J(u^o) + 2\,x(u^o)^T A x_u (u - u^o) + (u - u^o)^T x_u^T A x_u (u - u^o)$$

Knowledge of the gradient matrix $x_u = \frac{\partial x}{\partial u}$ (nxm) at u^o is sufficient to determine the globally minimizing u^o:

$$u^o = u - (x_u^T A x_u)^{-1} x_u^T A x(u)$$

The iteration procedure implements this solution by adding one component to a running estimate of u^o with each computation of x. The result is essentially a reduction scheme for inverting $x_u^T A x_u$ while computing one column of x_u at each stage of the reduction.

Relative to more general second-order methods, the procedure can be very efficient. This is especially true when the relation of x to u requires lengthy computation, since the solution is produced from only m+1 computations of x. For each computation of x, the procedure both adds one component to the estimate of u^o and updates previously chosen components. Thus one is always as close to u^o as the information on x_u allows.

The reduction procedure is arranged in a geometrically appealing manner that allows one to evaluate the optimization. In particular, the method computes: (1) the relative importance of the various components of u in minimizing J; (2) the coupling between control components; and (3) the relative importance of different state components in determining u^o. As applied to the numerical design of a fixed configuration control system, this information allows one to make better choices of the free parameters and to reduce the number of states (errors) that need be considered. One additional feature is the ease with which additional components of u can be incorporated. This is also of some interest in the problem of maximum likelihood estimation, where u is the vector to be estimated.

Description of the Method

The method is based on two facts. The first of these is that a function of two variables, $J(u_1, u_2)$, can be minimized by: (1) finding the value of u_1, as a function of u_2, that makes J stationary with respect to u_1; (2) using this function to substitute for u_1 in J and obtain a new function, $J^1(u_2)$, that depends only on u_2; (3) finding the value of u_2 that makes $J^1(u_2)$ stationary with respect to u_2; and (4) then determining u_1 from the function of (1). This procedure is equivalent to setting the partial derivatives, J_{u_1} and J_{u_2}, simultaneously to zero, and it can be extended to any number of parameters. The second fact is peculiar to the present problem. Because J is quadratic in u, the optimizing component of u at any step in the above sequence is linearly related to the subsequently chosen components. Thus the substitutions of step (2) above produce problems of identical form in which the order of the optimization is successively reduced by one.

The sequence of computations is illustrated in Fig. 2 for three parameters. Two trial control vectors ($u^1 = \left[u_1^1, u_2^1, u_3^1\right]^T$ and u^2) are presented. An initializing computation of x is then made for $u = u^1$ (point 1 of Fig. 2). u_1 is then changed to u_1^2 and x re-computed (point 2). These computations yield approximate values of $x_{u_1} = \frac{\partial x}{\partial u_1}$ $(n \times 1)$ and allow one to compute the value of u_1 that makes $J_{u_1} = 0$. This optimizing value of u_1 is a linear function of u_2 and u_3 which can be denoted as $u_1^o(u_2^1, u_3^1)$ for $u_2 = u_2^1$ and $u_3 = u_3^1$ (point 3). The values of x at point 3 can be found by an interpolation of the values at 1 and 2. A new computation of x at point 4, where u_2 has been changed to u_2^2, then gives x_{u_2}. Now using the values of both x_{u_1} and x_{u_2}, one can determine the line in the u_3 u_3^1 plane along which u_1 is optimum (3-5'). This allows one to predict directly the minimizing point 5, where $u_2 = u_2^o(u_3^1)$ and $u_1 = u_1^o\left[u_2^o(u_3^1), u_3^1\right]$. After interpolating to find the corresponding values of x at 5, the computation of x at 6 yields successively: x_{u_3}; the line 5 - 7', along which both u_1 and u_2 are optimum for any choice of u_3; the optimum control vector at point 7; and the optimal state, $x(u^o)$, and minimum cost, $J(u^o)$. Finally, an actual computation of x and J at the predicted u^o provides a useful check on the assumption of linearity. It is also desirable in practice to select u^1 and u^2 to bracket u^o and to perform the optimization in the order of decreasing control importance.

One other feature of the method is a geometric picture of the way in which each state component affects the choice of u^o. Referring to Fig. 3, the best u_k for each single x_i is the value u_{k_i} at which x_i crosses zero. The overall u_{ok} is a weighted sum of these u_{k_i} with the weighting factors determined by the relative slopes of the x_i vs u_k lines. If all u_{k_i} are close together, u_k is an effective control component, and the parabolic curve for J has a lower minimum.

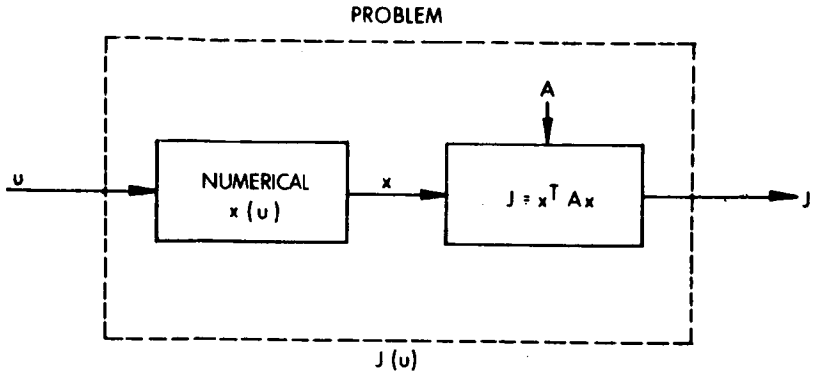

FORMAL SOLUTION

$$u^{o} - u = -(x_u^T A x_u)^{-1} x_u^T A x(u)$$

Fig. 1

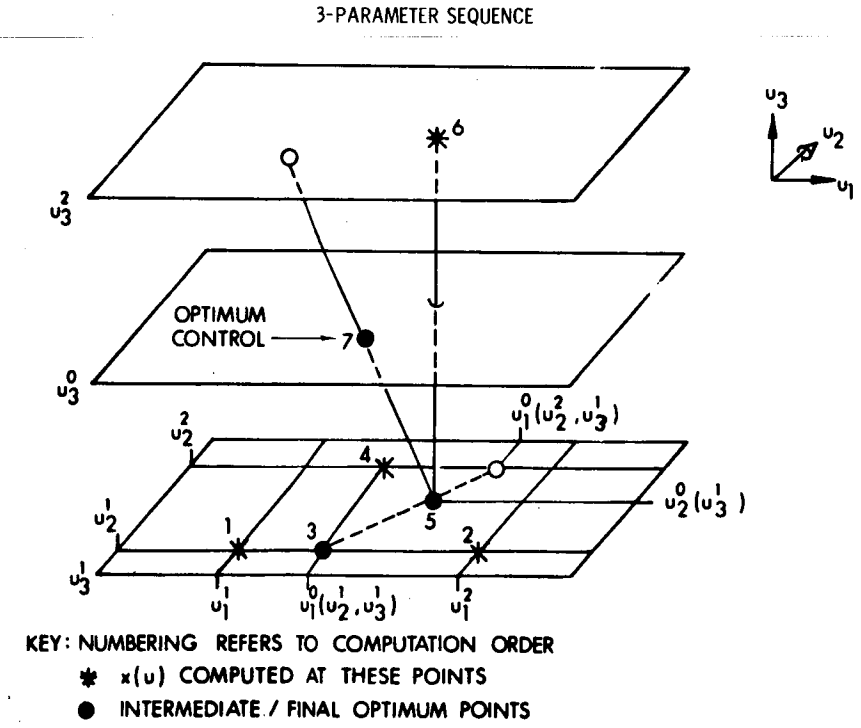

Fig. 2

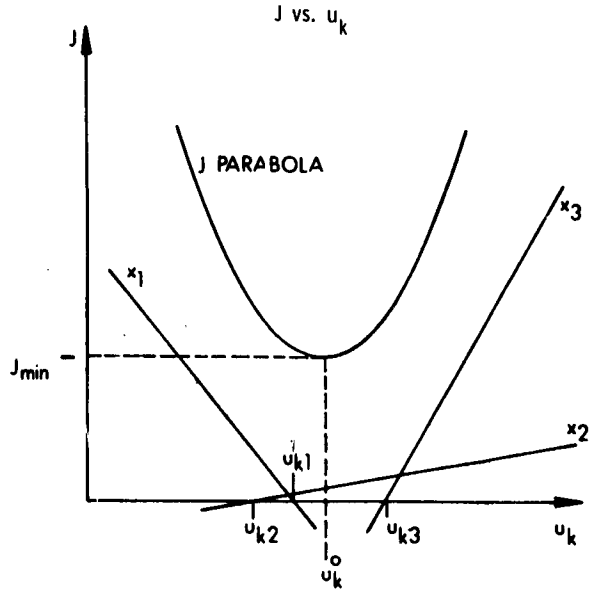

Fig. 3

APPLICATIONS

A. SOLUTION OF SIMULTANEOUS EQUATIONS

B. SELECTION OF GUIDANCE COEFFICIENTS

$$J = \overline{\Delta R^2} = \sum_{i=1}^{n} R_i^2 \, \sigma_i^2$$

$$R_i(u) = R_i(u^0) + \sum_{j=1}^{m} \left. \frac{\partial R_i}{\partial u_j} \right|_{u_0} (u_j - u_j^0) + \ldots$$

$$x = \begin{bmatrix} R_1 \\ \vdots \\ R_n \end{bmatrix} \quad ; \quad A = \begin{bmatrix} \sigma_1^2 & & 0 \\ & \ddots & \\ 0 & & \sigma_n^2 \end{bmatrix}$$

C. MAXIMUM LIKELIHOOD ESTIMATION

$$z = h(x) + v$$

$$J = v^T R^{-1} v \quad \text{with} \quad v = z - h(x)$$

Fig. 4

Applications

An obvious and exact application of the procedure is in the solution of sets of linear algebraic equations. It appears that this method of matrix inversion (or pseudo-inversion) can be made relatively free of numerical difficulties, and it is recommended that this be studied further. More generally, it is reasonable to expect the assumption of linearity to characterize problems in which a large number of states are traded off by choice of relatively few controls.

A problem which motivates this work is the selection of ballistic missile guidance coefficients. The design goal is to choose as few free parameters as possible and yet meet a specified terminal accuracy in the presence of various powered flight disturbances. Additionally, it is desirable to eliminate from consideration all disturbances which do not effectively contribute to the values of u^o. The cost function for this problem can be taken as the mean-squared range error:

$$J = \sigma_R^2 = \sum_{i=1}^{n} R_i^2 \sigma_i^2$$

where σ_i^2 is the variance of the i^{th} disturbance (e.g., per cent deviation in first stage mass flow rate) and R_i is the sensitivity of the range error to this disturbance; the value of R_i (that is x_i) can be a remarkably linear function of the free parameters (u). This problem is a good example of a complex relation between x and u since the computation of each component of x requires a complete simulation of the missile and guidance system, x itself requiring n+1 simulations for each u.

Another application of the procedure is in the problem of linearized maximum likelihood estimation. Consider measurements z made on an unknown constant x with additive, Gaussian noise (v):

$$z = h(x) + v$$

With x unknown, the maximum likelihood estimate of x is found by minimizing:

$$J = v^T R^{-1} v$$

where R is the covariance matrix of v and $v = z - h(x)$. (Here x is the "control" and v is the "state"). The interesting features of the method in this problem are the numerical determination of $H = \frac{\partial h}{\partial x}$ and the ease with which the dimension of the estimate can be increased.

CHAPTER IX

CLOSED LOOP "OPTIMAL" GUIDANCE EQUATIONS FOR SOFT LANDING

by

Charles F. Price

Much has been written on the subject of spacecraft soft landing trajectories over an atmosphereless celestial body, in particular the Earth's moon. The task of accomplishing a landing from a parking orbit about the moon has been posed as consisting of essentially two parts - an initial deboost phase, in which most of the space vehicle's velocity is eliminated, and a terminal phase during which the actual landing is effected[1].

During the deboost phase conservation of fuel is of prime importance, and the minimum fuel optimization problem with variable thrust magnitude and direction has been solved(Ref 1). The optimal trajectory has the usual characteristic that the thrust operates only at its maximum and minimum limits.

For the terminal phase, minimal fuel may not be the main consideration because the "jerky" maneuver associated with bang-bang thrust is an undesirable working environment for the astronauts just before touchdown. Furthermore, because the optimal maneuver usually requires maximum thrust at the end of the trajectory, the terminal state errors are very sensitive to the timing of the final thrust application. A requirement in this phase is that the astronauts have the capability of selecting visually a landing site; to accomplish this, the vehicle's attitude must be controlled so that possible landing sites can be viewed. A closed-loop control is necessary for precise acquisition of the landing site; therefore analytic guidance equations are desirable to limit the amount of computation. Accomplishing these objectives during the terminal phase of the descent trajectory is the subject of this study.

Two analytic control techniques that lead to smooth trajectories have been described by Bryson [2] and Klumpp [3].

Bryson formulates an optimization problem for a spacecraft moving in a constant gravitational field. The performance criterion is that the cost function

$$J = \frac{1}{2}\left[c_v \bar{v}\cdot\bar{v} + c_r \bar{r}\cdot\bar{r}\right]_{t=T} + \frac{1}{2}\int_{t_0}^{T} \bar{u}\cdot\bar{u}\, dt \qquad (1)$$

be minimized where $\bar{v}$, $\bar{r}$, $\bar{u}$, t_0, and T are, respectively, velocity and position with respect to a non-rotating coordinate frame fixed at the landing site, thrust acceleration, initial time, and a specified final time. The quantities c_v and c_r are weighting constants, and the integral term is referred to as the effort. The result is a linear, closed-loop control law producing a thrust variation having the form

$$\bar{u} = \bar{a} + \bar{b}t \tag{2}$$

where $\bar{a}$ and $\bar{b}$ depend on the initial state and the final time.

The approach taken by Klumpp is to require arbitrarily that $\bar{u}$ be a second-order polynomial in time.

$$\bar{u} = \bar{a}_1 + \bar{a}_2 t + \bar{a}_3 t^2 . \tag{3}$$

At any instant of time, the three vector coefficients $\bar{a}_1$, $\bar{a}_2$, and $\bar{a}_3$ are selected so that desired terminal values of the position, velocity, and acceleration vectors are achieved at a specified final time. No reference is made to minimization of a cost functional; the sole objective is to force a solution to the boundary-value problem. This objective can be achieved using many different functions, u(t). For example, $\bar{u}$ may be taken to be an exponential series, or time may be replaced by a different independent variable. The method, although it has led to successful guidance equations in specific applications, lacks the properties of a general theory for landing trajectory design because the form of the control is picked arbitrarily. Only the specified boundary conditions are met explicitly. The ultimate thrust equations depend upon additional criteria - e. g., fuel consumption, flight profiles, landing site visibility - that are not stated as boundary conditions. The result is that a trial and error approach in selecting control equations and examining simulated trajectories is required for each new application.

It is the purpose of this study to extend the optimization technique used by Bryson to develop guidance equations for a more general descent trajectory than has been considered previously. It is felt that this approach is more systematic than those in which the control is chosen arbitrarily, since the form of the guidance equations is dictated by the particular cost function to be minimized.

Optimization theory is not completely free of arbitrariness in determining the control. Although the cost functional is chosen to incorporate those trajectory characteristics that are to be optimized, its specific structure may be subjective. However, one is at least considering trajectory criteria such as fuel consumption, etc., before, rather than after, choosing the control.

The equations of motion for landing a vehicle on an atmosphereless planet

are approximately those of a body moving in a constant gravitational field $\bar{g}$, given by,

$$\dot{\bar{r}} = \bar{v}$$
$$\dot{\bar{v}} = \bar{g} + \bar{u} \tag{4}$$

The dynamical system treated in this discussion is that given by Eqs (4) augmented by the relations

$$\dot{\bar{u}} = \bar{u}_1$$
$$\dot{\bar{u}}_1 = \bar{u}_2$$
$$\vdots$$
$$\dot{\bar{u}}_n = \bar{u}_{n+1} \tag{5}$$

where $\bar{u}$, $\bar{u}_1$, ..., $\bar{u}_n$ are regarded as state variables whose boundary conditions may be specified and $\bar{u}_{n+1}$ has the status of the control variables. By specifying terminal values of $\bar{u}$ and its derivatives, terminal values of thrust magnitude, vehicle attitude, attitude rate, etc., can be controlled. We shall refer to $\bar{x}$ as the state, composed of $\bar{r}$, $\bar{v}$, $\bar{u}$, $\bar{u}_1$, ..., $\bar{u}_n$. A cost function of the general form

$$J_1 = \int_{t_0}^{t_f} \left[\bar{q}' \underline{R} \bar{q} + W_2 \bar{u} \cdot \bar{u} + \bar{u}'_{n+1} \underline{W}_1 \bar{u}_{n+1} + W_3 \right] dt \tag{6}$$

is considered where $\underline{W}_1$ is a positive definite 3x3 matrix, $\underline{R}$ is a positive semi-definite 3n x 3n matrix, W_2 is a positive constant, W_3 is constant, $\bar{q}' = (\bar{u}'_1, \bar{u}'_2, \ldots, \bar{u}'_n)$, and the prime of a vector denotes its transpose. In Eq (6) the integral terms involving $\bar{q}' \underline{R} \bar{q}$ and $\bar{u}'_{n+1} \underline{W}_1 \bar{u}_{n+1}$ are identified with the smoothness of the trajectory; the integral of $\bar{u} \cdot \bar{u}$ is a measure of the fuel consumed; and, with the appropriate terminal boundary conditions, the quantity

$$\int_{t_0}^{t_f} W_3 \, dt = (t_f - t_0) W_3$$

is a measure of the time available for an astronaut in the landing vehicle to view the landing site.

For specified t_f, the necessary conditions for minimizing J_1 subject to Eqs (4) and (5), the desired terminal conditions, and particular initial conditions, include a system of linear time-invariant differential equations that must be solved.

These equations can be integrated analytically in terms of the system's natural frequencies that are roots of the associated characteristic polynomial. One requirement for rapid closed-loop generation of the control equation is that the characteristic polynomial be such that its roots can be rapidly calculated. This requirement leads to consideration of somewhat specialized forms of J_1. For instance, the function

$$J_{11} = \int_{t_0}^{t_f} (\bar{u}_{n+1} \cdot \bar{u}_{n+1} + W_2 \bar{u} \cdot \bar{u} + W_3)\, dt \tag{7}$$

contains a less complex measure of smoothness than Eq (6); the characteristic polynomial associated with Eqs (4) and (5) and the minimum of J_{11} is factorable analytically. Preliminary results indicate that this simplified cost function leads to trajectories that may be acceptable for lunar landing applications. For the sake of definition let $\bar{u}^*_{11}(t)$ be the particular thrust function which minimizes J_{11} subject to the dynamic constraints.

Another consideration of importance is the selection of the final time t_f. The optimal choice is that value which minimizes the cost function. With this criterion, the expression that defines the optimal final time, t_f^*, is

$$H\left[t_f^*, \bar{x}^*(t_f^*), \bar{u}^*_{n+1}(t_f^*), \bar{\lambda}^*(t_f^*)\right] = 0 \tag{8}$$

where H is the Hamiltonian as a function of the optimal final time, final state $\bar{x}^*(t_f^*)$, final value of the optimal control, and final costate, $\bar{\lambda}^*(t_f^*)$. As a practical matter Eq (8) is difficult to solve for t_f^*, even for a functional as simple as J_{11} in Eq (7), because H is transcendental in t_f^*. Hence it may be expedient to introduce a method for determining t_f more amenable to on-board, closed-loop computation, but one which has some of the properties of the optimal technique.

One procedure that seems to yield satisfactory results is that of determining t_f from a simplified optimal control problem. For example, if J_{11} in Eq (7) is the cost function, let

$$J_{12} = \int_{t_0}^{t_f} \bar{u}_{n+1} \cdot \bar{u}_{n+1}\, dt \tag{9}$$

and find the thrust, $\bar{u}^*_{12}(t)$, which minimizes J_{12} for <u>fixed</u> t_f, subject to Eqs (4) and (5) and the desired boundary conditions. Now $\bar{u}^*_{12}(t)$ is a function of t_f; let t_f be chosen so that the function

$$F = \int_{t_0}^{t_f} \left[\bar{u}_{12}^{*}(t) \cdot \bar{u}_{12}^{*}(t) + \frac{W_3}{W_2} \right] dt \qquad (10)$$

is minimized. The forms of J_{12} and F are motivated by the desire to retain "some" of the structure of J_{11} in Eq (7); however, observe that t_f is chosen to minimize a function, not a functional. The relation

$$\frac{\partial F}{\partial t_f} = F'(t_0, t_f, \bar{x}_0, \bar{x}_f) = 0 \qquad (11)$$

where $\bar{x}_0$ and $\bar{x}_f$ are, respectively, the initial and terminal values of the state, and can be relatively easily solved for $t_f = t_{f,12}$.

The quantity $t_{f,12}$ is substituted for t_f in Eq (7) and the optimization problem associated with J_{11} is solved for the optimal thrust $\bar{u}_{11}^{*}(t, t_{f,12})$, emphasizing the dependence on $t_{f,12}$. The thrust $\bar{u}^{*}(t, t_{f,12})$ is linearly related to the present and desired terminal states by an expression of the form

$$\bar{u}_{11}^{*}(t, t_{f,12}) = \underline{K}_1(t, t_{f,12})\bar{x}(t) + \underline{K}_2(t, t_{f,12})\bar{x}_f \qquad (12)$$

where $\underline{K}_1$ and $\underline{K}_2$ are time-varying matrices whose elements are expressed in terms of elementary functions of time.

A summary of the steps required to generate $t_{f,12}$ and $\bar{u}_{11}^{*}(t, t_{f,12})$ is as follows:

1. Find $\bar{u}_{11}^{*}(t, t_f)$ as a literal function of t_f that minimizes some function J_{11} subject to the dynamic constraints.
2. Find $\bar{u}_{12}^{*}(t, t_f)$ as a literal function of t_f that minimizes a functional J_{12}, which is a simplified version of J_{11}, subject to the same dynamic constraints as in step 1.
3. Pick $t_f = t_{f,12}$ to minimize a function F which is related to J_{11} and $\bar{u}_{12}^{*}(t, t_{f,12})$.
4. Use the value of $t_{f,12}$ from step 3 for t_f in step 1 to generate $u_{11}^{*}(t, t_{f,12})$.

Equation (12) provides a closed-loop computation for $\bar{u}_{11}^{*}$, given $t_{f,12}$; however, Eq (11) does not constitute a closed-loop computation for $t_{f,12}$ and cannot be made so by replacing t_0 and $\bar{x}_0$ with t and $\bar{x}(t)$. This is true because $t_{f,12}$ is not a truly optimal value for t_f; it has been chosen by minimizing a function rather than a functional.

A variational method for adjusting $t_{f,12}$ in a discrete closed-loop fashion has been devised. The procedure uses the value of $t_{f,12}$ at time t_0, $t^0_{f,12}$, and the associated open-loop thrust $\bar{u}^*_{11}(t_0, x_0, t^0_{f,12}, t)$ to generate a nominal trajectory, $\bar{x}^*_0(t_0, \bar{x}_0, t^0_{f,12}, t)$, analytically.*

At a later time, $t_1 > t_0$, the state $\bar{x}(t_1)$ is measured and compared with the calculated nominal value $\bar{x}^*_0(t_0, \bar{x}_0, t^0_{f,12}, t_1)$, the difference being $\Delta x(t_1)$. A correction $\Delta t^1_{f,12}$ to $t^0_{f,12}$ is determined based on $\Delta x(t_1)$ and the requirement that the first order change in F' in Eq (11) at time t_1 caused by a deviation from the nominal trajectory be zero. The change in F' caused by progress along the nominal is ignored. A correction to $t^0_{f,12}$ to account for changes in the desired terminal state (landing site) can be computed by the same method. By calculating these corrections at times t_0, t_1, . . . t_j, . . . , a sequence of values $t^i_{f,12}$, given by

$$t^i_{f,12} = t^{i-1}_{f,12} + \Delta t^i_{f,12} \tag{13}$$

is generated, providing discrete, closed-loop computation of $t_{f,12}$.

* The closed-loop thrust, $\bar{u}^*_{11}(t, t^0_{f,12})$, in Eq (12) is applied to the vehicle.

REFERENCES

1 Berman, Lawrence J., "Optimum Soft Landing Trajectories", 12th International Astronautical Congress, 1963, Academic Press, New York.

2 Bryson, Arthur E., Jr., "Linear Feedback Solutions for Minimum Effort Interception, Rendezvous, and Soft Landing", AIAA Journal, August 1965, Vol 3, No. 8.

3 Klumpp, Allen, "A Manually Re-targeted Automatic Descent and Landing System for LEM", AIAA/JACC Guidance and Control Conference, Seattle, Washington, August 15-17, 1966.

CHAPTER X

THE TWO-PLANET FLYBY PROBLEM

by

Ronald Eng Young

The two-planet or double flybys to be considered in this report are a version of the "interplanetary grand tour" which departs Earth, passes by Mars and Venus once each without stopover, and returns to Earth. Such flybys were first studied in 1956 by Crocco, who simplified the problem by ignoring planetary orbit inclinations and gravitational perturbations. Battin, in 1959, found solutions without these simplifications, but suggested that launch windows might be as short as a few days. Gillespie and Ross in 1961 and Dixon in 1962 on the EMPIRE investigation also studied double flybys.

In our study at the Experimental Astronomy Laboratory we considered impulsive patched-conic trajectories flying by Venus and Mars in either order. The vehicle was launched from circular orbit about Earth and returned in an atmospheric entry to Earth. Heliocentric transfers were determined by solving Lambert's problem. At the flyby planets, the required thrust for the turn was computed as the velocity difference between the inbound and outbound hyperbolae at the common peripoint.

In the case of pure double flybys, for which no thrust is applied at the flyby planets, two of the four planet dates become dependent variables. However, even when the two independent dates are specified, the pure double flyby is not necessarily unique. The determination of the pure double flyby is in fact an exceedingly difficult problem, complicated by a non-planar solar system and the non-analytic matching of conic sections between solar and planetary frames.

We experimented with a number of algorithms in order to obtain the one most suitable for finding pure double flybys. We initially investigated the region in the vicinity of a known pure double flyby solution found by Battin[1]. We held the Earth-launch and Earth-arrival dates fixed and plotted the data shown in Fig. 1. The sum of velocity increments includes that of launch from Earth orbit and those required at the two flyby planets. Note that the intersection of the two pure flyby loci, which corresponds to the pure double flyby, lies near the minimum total Δv.

A necessary condition for pure flyby at a planet is that inbound and outbound

[1]Battin, R. H., Astronautical Guidance, pp. 169-172, Mc Graw-Hill Book Company, Inc., New York, 1964.

CONTOURS OF $\Sigma\Delta V$ AS FUNCTION OF T_{φ} AND $T_{\sigma'}$
FOR EARTH LAUNCH 244 1480 FOR EARTH ARRIVAL 244 1940

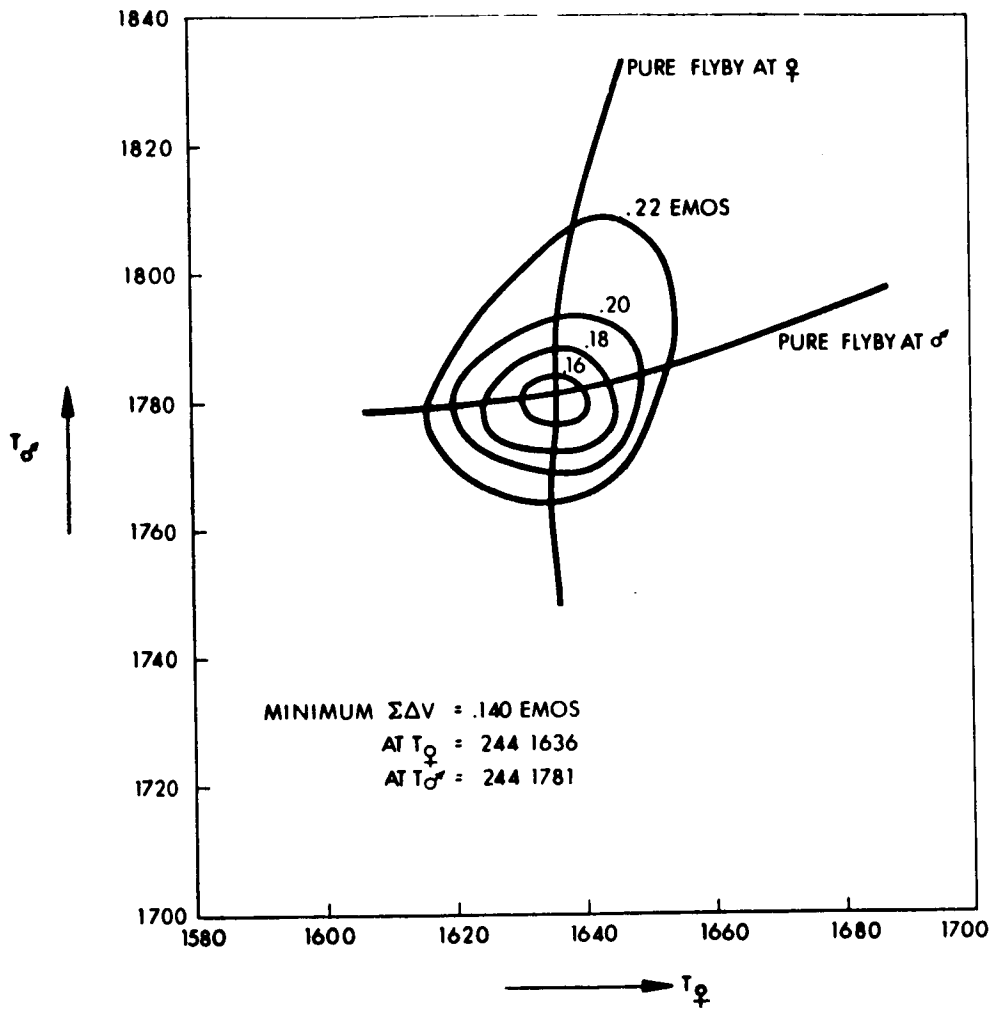

Fig. 1

velocity magnitudes in the planet frame be equal. A computer program was therefore created to select Venus and Mars flyby dates by iterating the velocity differences to zero. In this way the data shown in Fig. 2 was generated for Earth launch and arrival dates in the region of Battin's solution. The launch window is about forty days; the Earth arrival date may also take on a forty day range. Note that irrespective of the Earth dates chosen, the pure flyby date at Venus varies by only three days.

The program was used to search for pure double flybys during other Mars oppositions in the 1970's and 1980's. It was generally found that either the iteration did not converge or that the vehicle was required to pass below the surface of one or both flyby planets. To understand why the algorithm failed, we re-examined the data of Fig. 1 over a broader region. The result, shown in Fig. 3, displays not only the intersection corresponding to Battin's solution, but also five others. These five all correspond to pure double flybys passing below the surface of one or both flyby planets. Thus one can see that only a fortuitous choice of initial Mars and Venus dates allowed the programed iteration scheme to succeed in generating the data shown on Fig. 2.

We then tried a number of other algorithms in order to determine the Mars and Venus flyby dates for specified Earth launch and arrival dates; none of these other methods were successful. We eventually concluded that it would be best to make the Earth launch and arrival dates dependent variables so that a pure double flyby could be obtained.

In the search algorithm that finally evolved, we first choose the flyby dates at Venus and Mars. This decouples the Earth-launch leg from the Earth-arrival leg. We next cycle the Earth-launch date to obtain a pure flyby at the first flyby planet, and cycle the Earth-arrival date to obtain a pure flyby at the second flyby planet. We then repeat the procedure for all Venus and Mars dates of interest.

When a computer program using this algorithm was run over the time period 1970-2000, pure double flybys were found during every Mars opposition. A set of these pure double flyby dates from an opposition of interest could be used as initial conditions for the original program in order to map the Earth launch and arrival windows as in Fig. 2.

Our computations were carried out using the time-sharing system at the M. I. T. Computation Center. Since our work required a great deal of experimentation, we were able to make good use of the on-line program modification and debugging features of time-sharing. We set up flexible input and output formats so that we could conveniently examine data on-line. We could interrupt the program to terminate the run, change inputs, or change the algorithm. Thus we could make

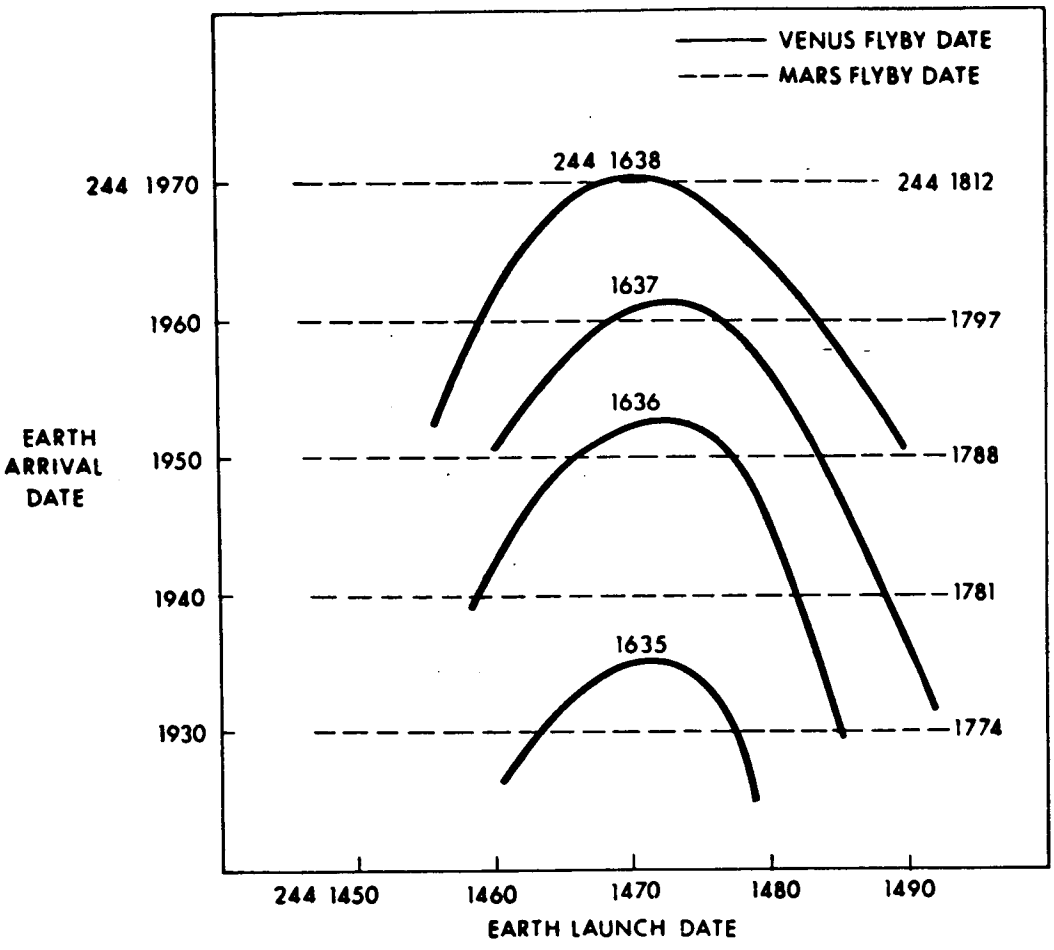

Fig. 2 Earth launch and arrival windows for pure flyby.

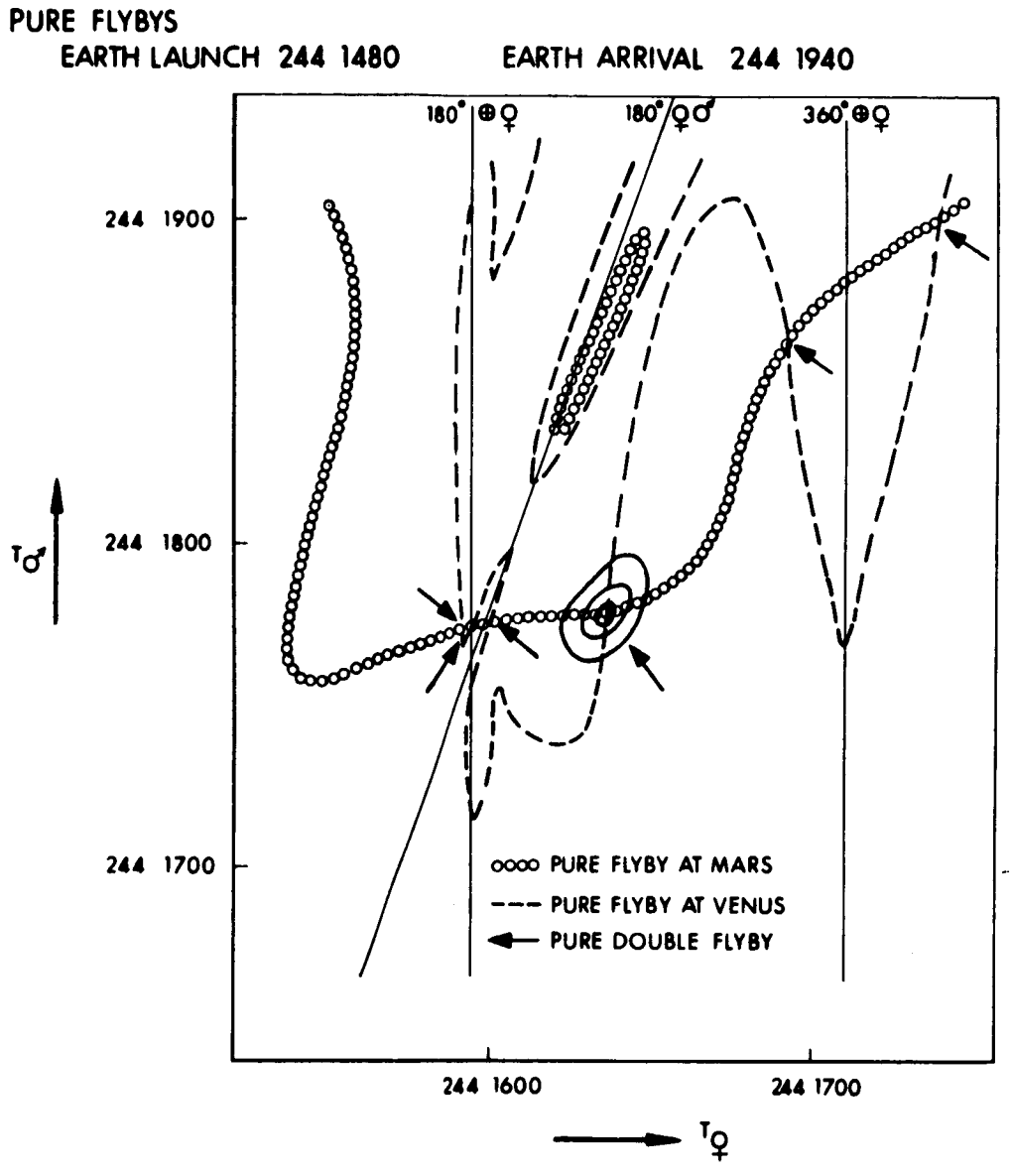
PURE FLYBYS
EARTH LAUNCH 244 1480
EARTH ARRIVAL 244 1940
180° ⊕♀
180° ♀♂
360° ⊕♀
244 1900
244 1800
244 1700
T♂
PURE FLYBY AT MARS
PURE FLYBY AT VENUS
PURE DOUBLE FLYBY
244 1600
244 1700
T♀

Fig. 3

a manual interation in order to test an algorithm before implementing a program modification. We could also run the program for data on specific trips in conjunction with the NASA Planetary Flight Handbooks, filling in gaps of coverage where necessary.

In conclusion, interplanetary mission planning involves a class of problems in which one experiments with computational algorithms quite often. We have been able to use time-sharing to good advantage in developing a fruitful method for obtaining profiles of one such mission: the pure double flyby.

CHAPTER XI

GYROCOMPASS SPACECRAFT ATTITUDE REFERENCE

by

William T. McDonald

The feasibility of using an IMU gyrocompass as a spacecraft attitude reference has been studied. The results have been reported in detail in reference 1 and a general description of the space gyrocompass system can be found in reference 2. The use of a gyrocompass for spacecraft attitude reference has been considered previously (reference 3) for near-Earth satellites, but the application to deep space vehicles has not, to the writer's knowledge, been previously reported. The essential result of the study is that a gyrocompass can be used for interplanetary missions. The study led to an adaptive system in which the gyrocompass gains vary with the measured orbital angular velocity.

Gyrocompassing in space is quite analogous to fixed-base gyrocompassing at the Earth's equator, as Fig. 1 illustrates. The Earth-based system tracks the gravity vector and the earth rate vector, while the space system tracks the line-of-sight to the reference body (Sun or planet) and the orbital angular velocity vector. The essential difference is that the earth rate is constant, while the orbital angular velocity varies greatly over an interplanetary transfer, ranging from approximately 40 earth rates during a planet swingby down to about 0.003 earth rate in the mid-course phase of a transfer to Mars or Venus. This large variation requires the system to be adaptive; the gyrocompass gains must change as a function of orbital angular velocity in order to satisfy stability and response requirements.

The configuration of the system is shown pictorially in Fig. 2 and schematically in Fig. 3. Sun/planet sensors replace the accelerometers on an Earth-based gyrocompass, but the configuration and signal flow in the space gyrocompass are otherwise quite analogous to the familiar Earth-based system. The Sun/planet sensor signals (the "level" errors) are processed in a digital computer, as shown in Fig. 3. The computer calculates the gyro torquing commands, and the gyrocompass gains according to the computational flow shown in the figure. Reference 1 contains a detailed derivation of these gain computation formulas, and it is shown there that the Z-loop (out-of-plane) gains K_{ZZ_1} and K_{ZZ_2} remain constant throughout the flight while the R and S loop gains K_{SR} and K_{SS} vary with the orbital angular velocity and the chosen values of natural frequency and damping factor for these

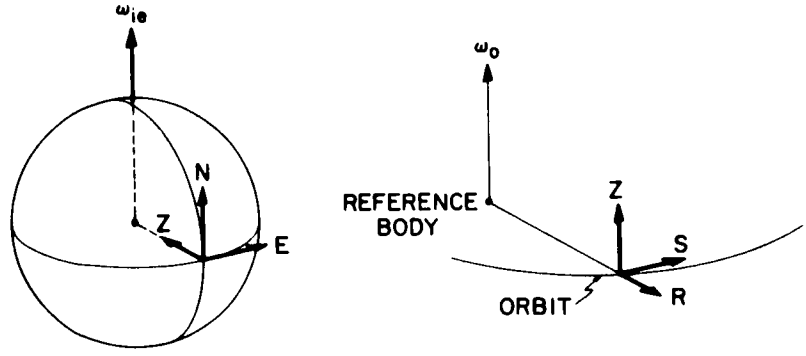

Fig. 1 Analogy between gyrocompassing on Earth equator and in orbit.

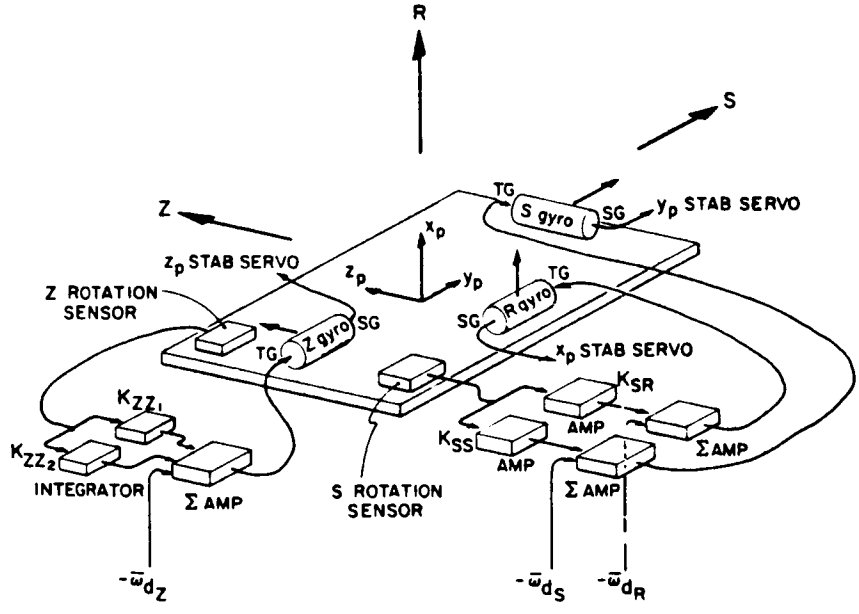

Fig. 2 Gyrocompass configuration.

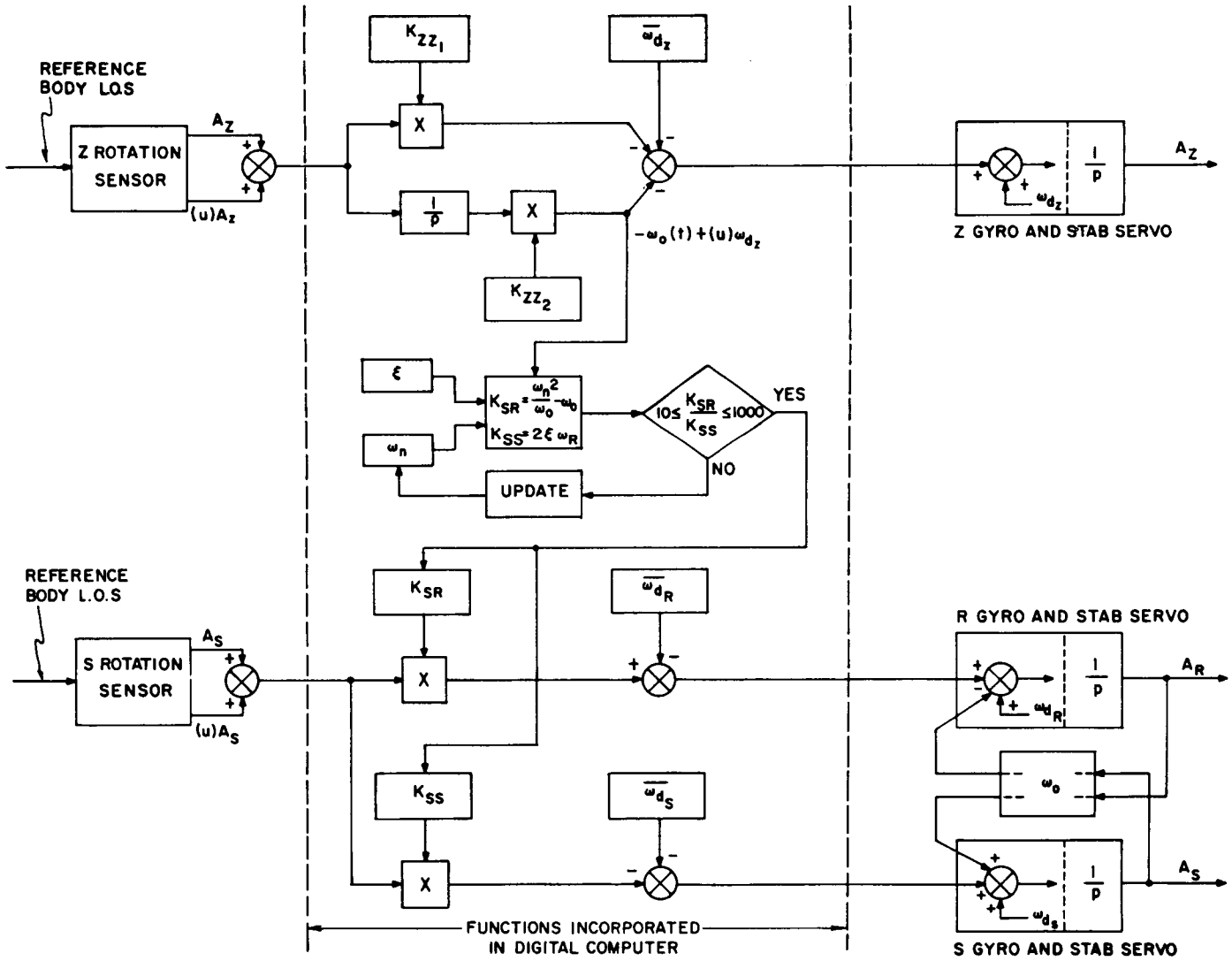

Fig. 3 Adaptive gyrocompass system mechanization.

coupled loops. The output signal from the K_{ZZ_2} integrator is a measure of the orbital angular velocity, and this is used in the adaptive gain computations as shown in Fig. 3. The design criterion for the choice of natural frequency and damping factor is that the system response to a disturbance shall damp out within a relatively short arc of the orbit. Hence, the natural frequency must be much greater than the orbital angular velocity.

Since the Z-loop provides a measure of orbital angular velocity for the gain computations, the Z-gyro must have a low drift rate (or the statistical model of its long-term drift behavior must be known if statistical filtering is to be used). Provisions can be made for in-flight gyro calibration by, for example, gyro wheel speed variation methods, platform multipositioning techniques, or statistical filtering.

The space gyrocompass system also has the capability of inflight erection and acquisition of the gyrocompass mode from a fully shut-down condition. The erection procedure is to acquire first of all the reference body (the Sun or a near planet) with the body trackers, and then to rotate the platform about the line of sight to the reference body until the Z-gyro is aligned with the orbital angular velocity vector. The platform tilt error about the Z-axis serves to indicate when the coarse alignment is achieved. After coarse alignment the system is placed in the gyrocompass mode and fine alignment then follows after the system settling time. This procedure is explained in more detail in reference 1. The time required for erection and alignment depends on the orbital angular velocity and varies from a few minutes in a near orbit about a planet to a few hours in a heliocentric transfer orbit between planets.

Reference 1 gives a detailed derivation of the sensitivity coefficients relating system misalignment errors to instrument errors. These sensitivity coefficients depend upon the magnitude of the orbital angular velocity and therefore vary throughout a non-circular orbit. This is particularly true of the gyro error sensitivity coefficients, which generally vary inversely with orbit angular velocity. In general the system alignment accuracy is highest in an orbit about a planet and lowest in midcourse phases. The actual accuracy expected of a gyrocompass cannot be stated without classified gyro performance data, but the error sensitivity coefficients show the trend of system accuracy. Table 1 shows the numerical values of these coefficients for gyrocompasses in a parking orbit about the Earth, in an Earth-Mars Hohmann transfer, and operating on the earth equator. It is evident that the gyrocompass accuracy is highest where it is most needed, in the vicinity of a planet where observational instruments require high pointing accuracy. In the midcourse phase where the system accuracy is lowest, the spacecraft orientation accuracy required is diminished. It is the writer's opinion that, when present-day gyro

Table I Typical Gyrocompass Error Sensitivity Coefficients

Sensitivity Coefficient	Planetocentric Parking Orbit *	Heliocentric Transfer Orbit **	Fixed-base Gyrocompass at Earth's Equator ***
Level sensor errors:			
$\partial A_R/\partial(u)A_S$	negligible	negligible	negligible
$\partial A_S/\partial(u)A_S$	1 $\widehat{\text{sec}}/\widehat{\text{sec}}$	1 $\widehat{\text{sec}}/\widehat{\text{sec}}$	1 $\widehat{\text{sec}}/\widehat{\text{sec}}$
$\partial A_Z/\partial(u)A_Z$	1 $\widehat{\text{sec}}/\widehat{\text{sec}}$	1 $\widehat{\text{sec}}/\widehat{\text{sec}}$	1 $\widehat{\text{sec}}/\widehat{\text{sec}}$
Gyro drift rate errors:			
$\partial A_R/\partial(u)\omega_{d_R}$	$0.7\frac{\widehat{\text{sec}}}{\text{meru}} = 47\frac{\widehat{\text{sec}}}{\text{deg/hr}}$	$83\frac{\widehat{\text{sec}}}{\text{meru}} = 5.8\times10^3\frac{\widehat{\text{sec}}}{\text{deg/hr}}$	$2\frac{\widehat{\text{sec}}}{\text{meru}} = 1.38\times10^2\frac{\widehat{\text{sec}}}{\text{deg/hr}}$
$\partial A_R/\partial(u)\omega_{d_S}$	$12.1\frac{\widehat{\text{sec}}}{\text{meru}} = 806\frac{\widehat{\text{sec}}}{\text{deg/hr}}$	$21\frac{\text{deg}}{\text{meru}} = 5\times10^6\frac{\widehat{\text{sec}}}{\text{deg/hr}}$	$206\frac{\text{sec}}{\text{meru}} = 1.38\times10^4\frac{\widehat{\text{sec}}}{\text{deg/hr}}$
$\partial A_S/\partial(u)\omega_{d_R}$	$0.02\frac{\widehat{\text{sec}}}{\text{meru}} = 1.4\frac{\widehat{\text{sec}}}{\text{deg/hr}}$	$0.03\frac{\widehat{\text{sec}}}{\text{meru}} = 2.2\frac{\widehat{\text{sec}}}{\text{deg/hr}}$	$0.01\frac{\widehat{\text{sec}}}{\text{meru}} = 0.7\frac{\widehat{\text{sec}}}{\text{deg/hr}}$
$\partial A_S/\partial(u)\omega_{d_S}$	negligible	negligible	0

*Circular Earth orbit at one planet radius

**Typical of an Earth-Mars Hohmann transfer, eccentricity ≈ 0.3

***An Earth-based gyrocompass of the configuration as the orbital system, but with gains set for Earth angular rate.

Note that all other sensitivity coefficients are identically zero.

capabilities are weighed against mission accuracy requirements, a gyrocompass can meet the accuracy requirements.

The important tradeoffs between gyrocompass and star tracker attitude reference techniques can be briefly summarized as follows:

1. The gyrocompass always aligns with instantaneous orbital coordinates RSZ (see Fig. 1). The spacecraft can then be held in an orientation fixed relative to the reference body. This can only be accomplished with a star tracker system if there is a pole star for each phase of the interplanetary transfer orbit.

2. The gyrocompass system reacts easily and automatically to changes in the orbit phase and reference body. Star tracker systems usually are constrained to keep the Sun as the reference body throughout a flight, even during the terminal phases near a planet.

3. The gyrocompass is not restricted to fly preplanned reference trajectories.

4. The gyrocompass appears to be a natural mechanization for low thrust trajectories in which the orbital plane and angular velocity change continuously and in which the thrust direction must be programmed relative to the instantaneous orbital plane and the radius to the reference body. The required changes of the reference body are also easily accommodated.

REFERENCES

1 W. T. McDonald, "An Adaptive Gyrocompass System for Attitude Reference on Interplanetary Trajectories," MIT Experimental Astronomy Laboratory Report **RE-21,** December 1965.

2 W. T. McDonald, "IMU Gyrocompass as Attitude Reference in Space," SPACE/AERONAUTICS, September 1966.

3 R. L. Gordon, "An Orbital Gyrocompass Heading Reference for Satellite Vehicle," AIAA Paper No. 64-238, 1st AIAA Annual Meeting, Washington D. C., June 29 - July 2, 1964.

CHAPTER XII

APPLICATION OF QUADRATURE FORMULAS TO ESTIMATION USING MOMENTS

by

Stephen J. Madden Jr.

The problem considered here is that of extracting certain information about a nondecreasing piecewise continuous function $\Phi(x)$ on the unit interval, given a finite number, N, of its moments, μ_n,

$$\mu_n = \int_0^1 x^n \, d\Phi(x) \qquad n = 0, 1, 2, \cdots N.$$

This could be a typical probability problem for instance. There are many alternatives to consider, such as substitution of the values of the moments into the moment generating function expansion to get an approximation to $\Phi(t)$ or an integral of it. The method employed here is constructive and it gives upper and lower bounds on the quantity $\Phi(x_0) - \Phi(0)$ throughout the interval $[0, 1]$. It may thus be used in probabilistic problems to estimate probabilities in a non-parametric fashion similar to that given by Chebyshev's theorem

$$P(|x - \mu| \geq \lambda\sigma) \leq \frac{1}{\lambda} 2.$$

The given moments are used to generate as many of the polynomials orthogonal with respect to $d\Phi(x)$ as possible. Assume that there are M of these polynomials and denote them by $\omega_n(x)$. These polynomials can then be used to generate two quadrature formulas for integrals with respect to $d\Phi(x)$ which allow one of the node points of the formula to be fixed in advance in $[0, 1]$. One of the formulas will always be of the highest degree of precision, and they can be given completely in terms of the two highest polynomials, $\omega_M(x)$ and $\omega_{M-1}(x)$. The degree of precision will be 2M - 2 and thus the quadrature formulas will be exact when applied to polynomials of this degree or lower.

Consider the difference $\Phi(x_0) - \Phi(0)$, where x_0 is a point in $[0, 1]$. We then have

$$\Phi(x_0) - \Phi(0) = \int_0^{x_0} d\Phi(x) = \int_0^1 H(x_0 - x) \, d\Phi(x),$$

where H (x) denotes the Heaviside step function. This last integral can be most conveniently described as the integral with respect to $d\Phi(x)$ of the Heaviside step function. For a given value of x_0, the nodes of the quadrature formula will be distributed throughout $[0, 1]$. Suppose that K nodes lie in the region to the left of x_0. We then construct the following polynomials, $P_U(x)$ and $P_L(x)$ both of degree 2M - 2. Specify that P_U and P_L are equal to $H(x_0 - x)$ at the node points $x_1 \cdots x_K$ and tangent to it there. Also specify that both polynomials are zero at the node points

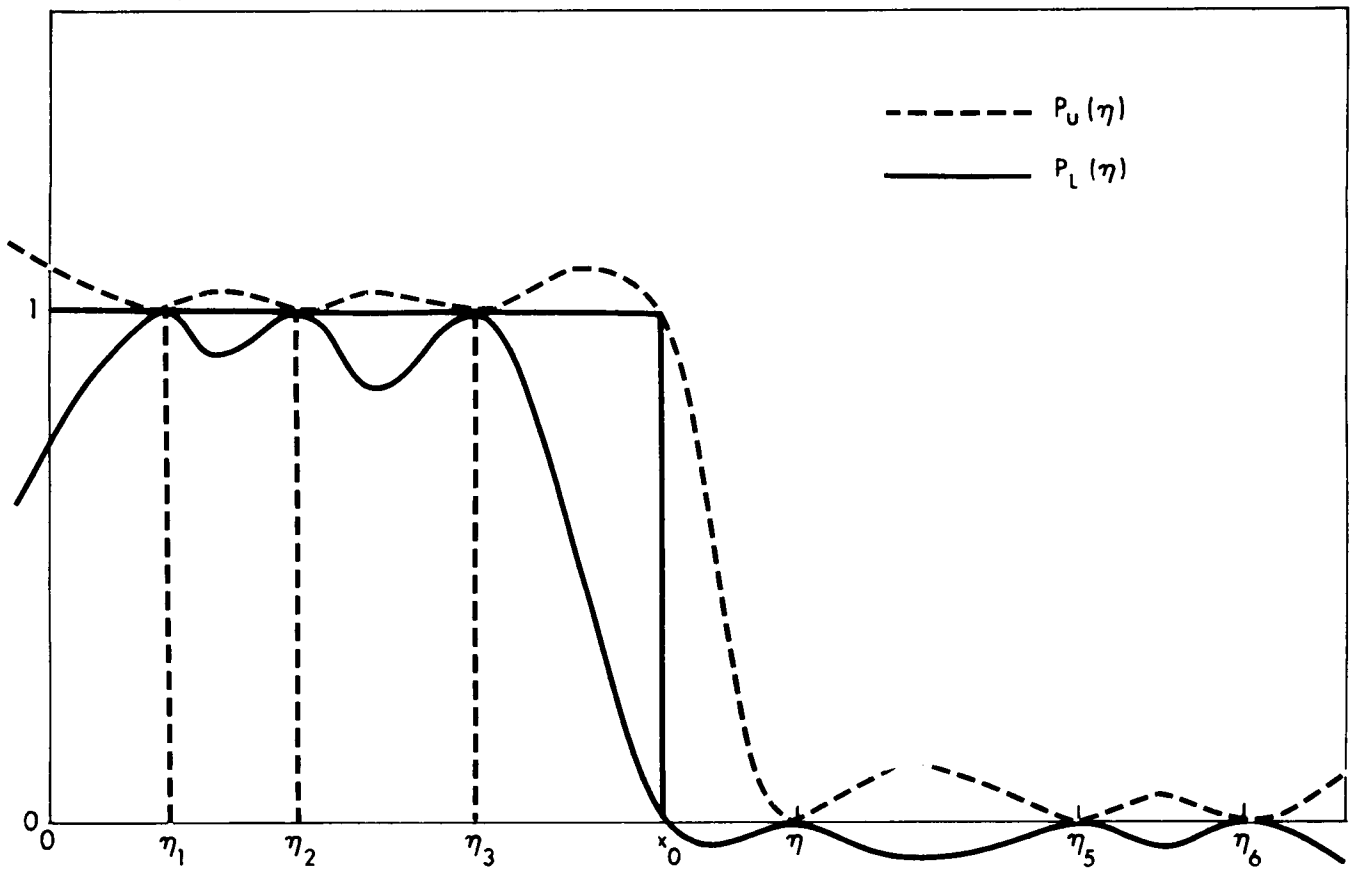

Fig. 1 Examples of the bounding polynomials.

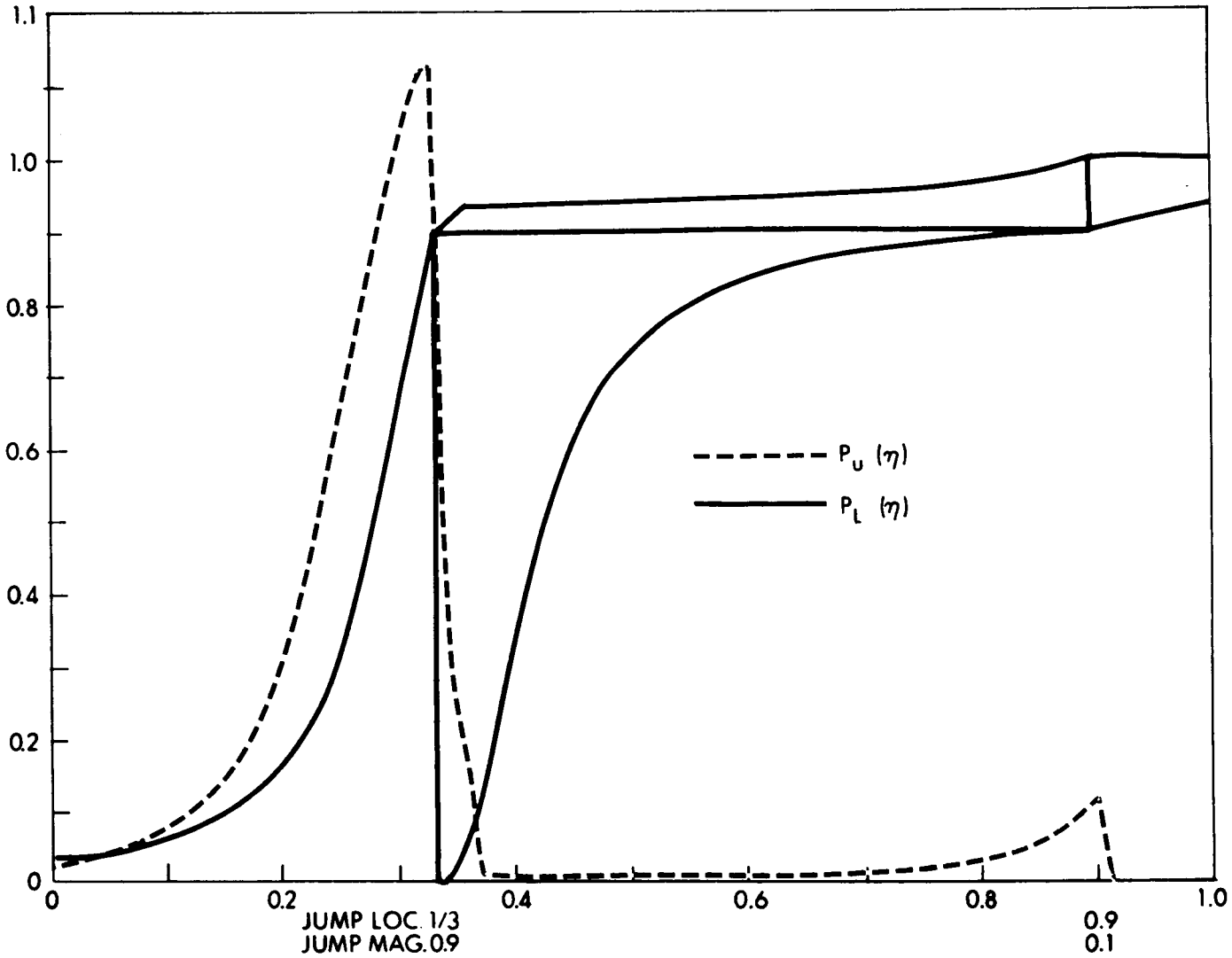

Fig. 2 Examples of bounds using three moments.

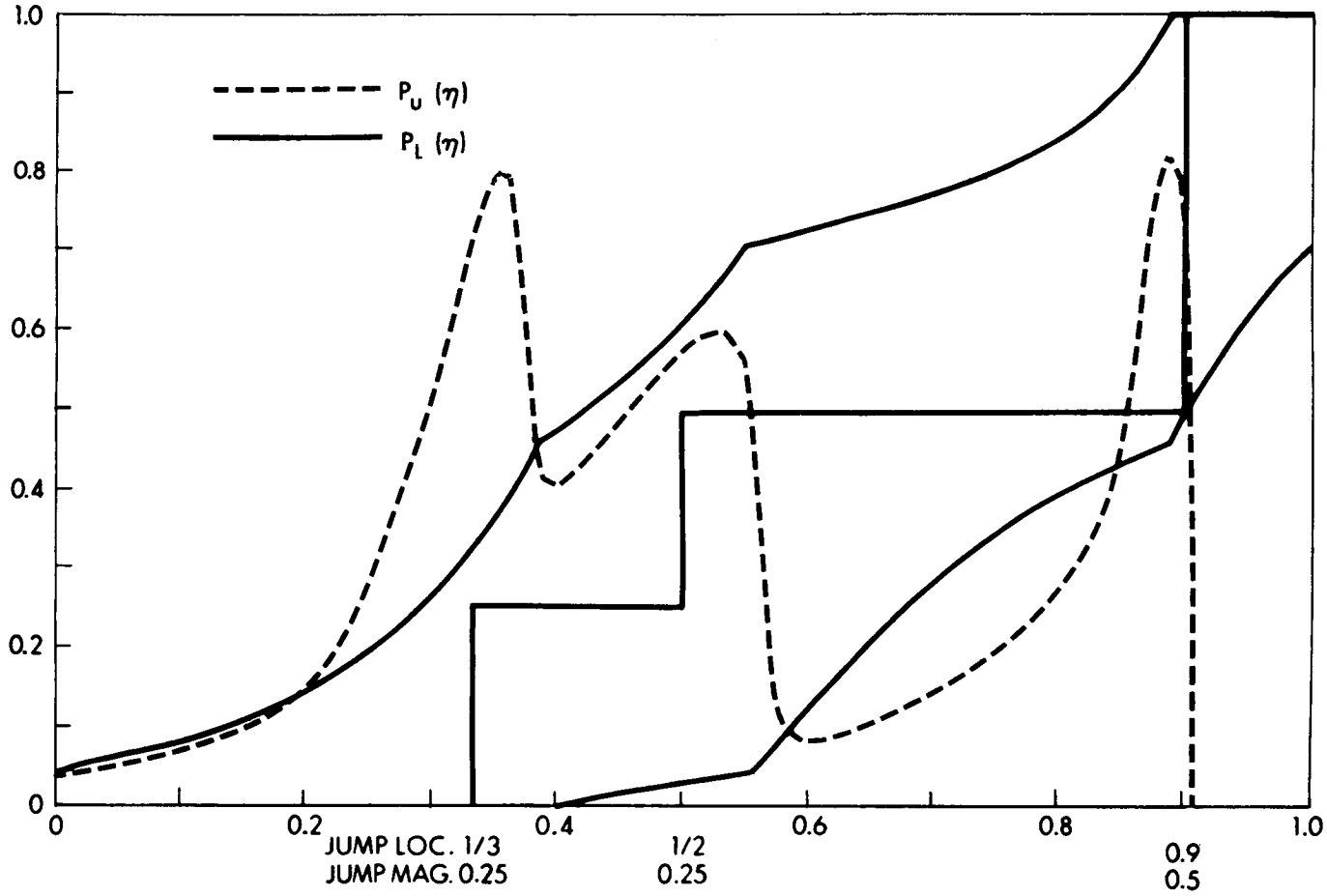

Fig. 3 Examples of bounds using three moments.

greater than x_0 and tangent to the x-axis there. Require that $P_U(x)$ pass through one at x_0 and that $P_L(x)$ pass through zero there. These conditions, and there are $2M - 1$ of them, specify the two polynomials uniquely. By their very construction we have (see Fig. 1)

$$P_U(x) \geq H(x_0 - x) \geq P_L(x)$$

and thus

$$\int_0^1 P_U(x)\, d\Phi(x) \geq \Phi(x_0) - \Phi(0) \geq \int_0^1 P_L(x)\, d\Phi(x).$$

The quadrature formula can be applied to both of these integrals and the results will be exact since the degree of both polynomials is $2M - 2$. The desired result follows since $P_U(x)$ and $P_L(x)$ can be constructed. Practically speaking, one never needs to construct them, since their values are known at the node points. The values of the integrals can be directly given in terms of $\omega_M(x)$ and $\omega_{M-1}(x)$.

To illustrate the procedure and its results, two simple functions have been chosen for $\Phi(x)$ and, using their first three moments, bounds have been generated. Both functions are step functions and they are displayed with their computed bounds in Figs. 2 and 3.

CHAPTER XIII

AN APPLICATION OF MATCHED ASYMPTOTIC EXPANSIONS TO HYPERVELOCITY FLIGHT MECHANICS

by

Captain Richard F. Willes, Asst. Prof., U.S. Air Force Academy, Colorado 80840

The method of matched asymptotic expansions has been established as a systematic means of treating a nonlinear problem in which a small parameter appears. It has been extensively used in the field of fluid mechanics [2] and recently in a number of problems in celestial mechanics. [3, 4] This paper describes a natural extention of the previous uses of the method into the area of entry dynamics or hypervelocity flight mechanics.

The method is introduced as a completely straightforward approach to the problem of analytically describing hypervelocity flight trajectories. Both new and previously known solutions to the flight dynamic equations are produced in a unified procedure that is capable of: (1) defining the solutions' region of validity; (2) extending the solutions to higher order in the small parameter; and, (3) combining the solutions to obtain solutions valid over several regions of interest.

The procedure involves finding all valid asymptotic first approximations to the dynamic equations of flight. All possible cases are exhausted by considering every possible value of the problem variables measured in powers of the problem's small parameters. Terms that may be neglected then appear multiplied by a power of the small parameter. The first, or lowest order, approximation for a particular range of value of the variables is obtained by simply retaining the non-negligible terms. The neglected terms are then included in higher approximations. As the solutions to the higher approximations are expressible in terms of the solution to the lowest order problem, the procedure may be logically continued to an arbitrarily high order and in principle the maximum possible accuracy can be achieved. Composite expansions, valid over several regions of interest, are produced by requiring that the appropriate expansions match in their region of common validity.

The object of this paper is to place the previous work in flight mechanics in this framework of systematic approximation. This allows a careful delineation of the range of validity and accuracy of new and existing solutions. It also offers a straightforward method of improving these solutions by extending them to higher order. Solutions uniformly valid over a number of regions are produced by matching and combining expansions.

Specifically, all regions of behavior of the dynamic equations for two-dimensional flight in a non-rotating atmosphere surrounding a spherically symmetric planet are exhaustively mapped, and the appropriate lowest order approximations to the dynamic equations are identified.

The analyses of Sanger [5], Allen and Eggers [6], Chapman [7], Lees [8], and Shen [9], are all shown to be systematic approximations within this context. The extent to which Loh's [10] analysis can be considered systematic is demonstrated. In fact, Loh's "second order" solution is shown to be a multiple regime "first order" approximation that can be corrected to a rational lowest order solution.

Higher order Allen and Eggers skip and ballistic trajectories are computed. An Allen and Eggers skip solution is matched with a Shen solution to produce a composite solution valid over a larger range than either of the individual solutions.

The problem of two-dimensional flight through a non-rotating atmosphere surrounding a spherically symmetric planet is shown to be systematically embedded in the problem of flight in a rotating atmosphere surrounding an oblate planet.

A method which permits analytical calculation of optimal entry trajectories and which uses this expansion technique and a discontinuous approximation to a real drag polar is suggested. The advantages of uniformly valid asymptotic expansions for guidance techniques are enumerated, and methods of performing explicit and linear nominal guidance with these solutions are illustrated.

Finally, the significantly different dynamic structure of entry trajectories into Mars and Titan as opposed to Earth, Venus, Jupiter, and Saturn are discussed.

The major contribution of this investigation is the demonstration of the usefulness of the method of matched asymptotic expansions as an analytical tool for investigating currently interesting problems in hypervelocity flight mechanics. Many interesting results are produced with a straightforward application of a well-established perturbation technique in an area in which analytical progress in the past has been difficult.

REFERENCES AND FIGURES

1 Willes, R. E., "An Application of the Methods of Matched Asymptotic Expansions to Ordinary and Optimal Problems in Hypervelocity Flight Dynamics," Ph. D. Thesis, Dept. of Aeronautics and Astronautics, M. I. T., Cambridge, Massachusetts, September 1966.

2 Van Dyke, M., Perturbation Methods in Fluid Mechanics, Academic Press, New York, 1964.

3 Lagerstrom, P. A., and Kevorkian, J., "Numerical Aspects of Uniformly Valid Asymptotic Approximations for a Class of Trajectories in the Restricted Three-Body Problem," Progress in Astronautics and Aeronautics, Vol. 14, Celestial Mechanics and Astrodynamics, Szebehely (Ed.), Academic Press, 1964.

4 Breakwell, J. V., and Perko, L. M., "Matched Asymptotic Expansions, Patched Conics and the Computation of Interplanetary Trajectories," AIAA Paper No. 65-689.

5 Sanger, E., Raketen-Flugtechnik, Berlin, 1933.

6 Allen, H. J., and Eggers, A. J., Jr., "A Study of the Motion and Aerodynamic Heating of Missiles Entering the Earth's Atmosphere at High Supersonic Speeds," NACA TN 4047, October 1957.

7 Chapman, D. R., "An Approximate Analytical Method for Studying Entry into Planetary Atmospheres," NACA TN 4246, May 1958.

8 Lees, L., Hartwig, F. W., and Cohen, C. G., "Use of Aerodynamic Lift During Entry into the Earth's Atmosphere," ARS Journal, September 1959.

9 Shen, Y. C., "Series Solution of Equations for Re-entry Vehicles with Variable Lift and Drag Coefficients," AIAA Journal, Vol. 1, No. 11, November 1963.

10 Loh, W. H. T., Dynamics and Thermodynamics of Planetary Entry, Prentice-Hall, 1963.

CHAPTER XIV

THE ROTATION OF THE PLANET MERCURY

by

Charles Counselman

1. Introduction

Radar observations of Mercury have disclosed that the sidereal period of the planet's axial rotation is 59 ± 3 days (Pettengill and Dyce, 1965; Dyce et al., 1966), rather than the previously accepted period of 88 days (see, for example, Dollfus, 1953). The purpose of our investigation is to discover the implications for our theories of the solar system (and of the inner planets in particular) which this new result may require.

A number of explanations of this new result have appeared. Peale and Gold (1965) immediately pointed out that the effect of solar tidal friction on the planet would be to produce an axial rotation rate lying between the orbital mean motion and the orbital rate at pericenter, because in an elliptic orbit the tidal interaction is strongest near pericenter, when the instantaneous orbital angular velocity is also greatest.

However, Colombo (1965) noticed that the observed spin period P_s was nearly two-thirds of the 88-day orbital period P_o and suggested that the axial rotation might be "locked" to the orbital motion in a three-halves resonance state by an additional solar torque due to triaxiality of the planet's inertia ellipsoid. Colombo and Shapiro (1965) examined a two-dimensional model of the Sun-Mercury interactions, considering both tidal drag and a torque due to a permanent axial asymmetry of the planet. This analysis, carried through the second order in orbital eccentricity, showed the possibility of torque balance with $P_s = \frac{2}{k} P_o$, $(k = 1 \rightarrow 4)$, provided that the tidal drag torque was sufficiently smaller than the torque due to axial asymmetry. By numerical integration with a relatively large assumed value for the tidal torque, they demonstrated that in the vicinity of the k = 3 resonance, the average rotation period P_s tended asymptotically to $\frac{3}{2} P_o$, under the action of the combined torques.

Goldreich (1965) also reanalyzed the arguments of Peale and Gold (1965), but did not consider the possibility of the axial rotation being locked to the orbital motion in a non-synchronous mode.

Goldreich (1966) further derived a criterion supposed to determine whether the final stable spin state of the planet would be synchronous (k = 2), or the non-synchronous rotation originally suggested by Peale and Gold (1965). The analysis, considerably simplified, yielded a simple inequality condition involving only the ellipsoid asymmetry (B - A)/C and the orbital eccentricity, e. Still no analytical consideration was given of commensurate spin states other than synchronous rotation.

Goldreich and Peale (1966a) reconsidered Mercury's rotation and reached essentially the same conclusions as had been drawn previously by Colombo and Shapiro (1965).

In addition to studying analytically the rotation in the neighborhood of resonance states, Bellomo, Colombo, and Shapiro (1966) considered the long-term evolution of Mercury's spin and the conditions for possible capture into the various states.

In a later paper Goldreich and Peale (1966b) calculated probabilities of spin capture into commensurate states, based on the assumption that as the planet approaches a possible resonance capture, the random variables of rotation angle and of rotation rate are independent.

2. Areas of Investigation

The various treatments of the axial rotation of Mercury published so far have left unanswered at least two important groups of questions. These are

I. Questions regarding the local stability of the three-halves resonance; and

II. Questions regarding the probability of Mercury being captured into the three-halves resonant spin state, assuming the original rotation of Mercury to have been rapid, in either a direct or retrograde sense, or with the axis inclined by a large angle to the normal to the orbit plane.

Because radar and recent optical observations indicate that the actual rotation period of Mercury cannot in fact be far from $\frac{2}{3} P_o$, the answers to these questions may allow useful inferences to be drawn about the past or future of the planet. The incompleteness of the existing rotation theory may also be revealed.

I. Local stability of the three-halves resonance.

In the vicinity of the three-halves resonance, the effect of the solar torque on the permanent axial asymmetry is to cause an oscillation of the value of the rotation rate about the resonance value. The frequency of this oscillation is proportional to the square root of the degree of asymmetry (B - A)/C, in the first approximation. To first power in the asymmetry, the oscillation is undamped in the absence of tidal drag. By invoking plausible

amounts of tidal friction (in terms of the believed behavior of the solid Earth), the oscillation is damped, but only very lightly. Decay time-constants on the order of 2×10^6 years are obtained. More detailed analysis may show that higher-order effects of the axial asymmetry torque, or of the periodic variation of orbital eccentricity due to planetary perturbations, are sufficient to alter seriously or upset this narrow margin of stability.

II. Probability of capture into the three-halves state.

Assuming this rotation to be asymptotically stable, and assuming the dynamics of capture to be completely known and accurately modelled, the probability of capture is a functional of the (assumed) a priori distribution of initial conditions at some time in the past. That is, some initial conditions lead to capture, and others do not. Shapiro (1966) has obtained results of numerical integration of the equations of motion for the model discussed by Bellomo, Colombo, and Shapiro (1966), starting from a sampling of initial conditions far from the resonance. Several values of (constant) orbital eccentricity and tidal-drag/permanent-deformation torque ratio have been investigated by him in this way. An analytic treatment is desired to understand these results and in order to generalize to other reasonable configurations of parameters. The effect of periodic and secular variations in these parameters (e.g., orbital eccentricity, Q^{-1} of the planet) must be investigated. Other parameters not included in the original model may prove decisive.

3. Analysis

Equations which accurately describe the rotation of even the most simple model of the planet are quite complex, owing largely to the relatively high eccentricity of Mercury's orbit. This eccentricity, which makes analysis tedious, gives rise to unorthodox features in the rotational motion, such as the existence of stable nonsynchronous but commensurate spin rates. Some qualitative understanding of the dynamics of rotation may be had, however, by studying the simplified differential equation obtained by Goldreich (1966).

Denoting the planet's principal moments of inertia by $A < B < C$, where C is the moment about the spin axis (assumed normal to the orbital plane), the orbital mean motion by n, and the instantaneous rotation angle between the planet's longer equatorial axis and the orbit semimajor axis by θ, we have approximately, in the vicinity of the k^{th} resonance ($\dot{\theta} \approx \frac{k}{2} n$),

$$\ddot{\theta} + \Omega^2 \sin 2 \left(\theta - \frac{k}{2} nt\right) = -T \qquad (1)$$

where

$$\Omega^2 \equiv \frac{3}{2} \frac{(B - A)}{C} f(k, e) n^2 \tag{2}$$

and

T = the tidal drag torque, which is in general a function of $\dot{\theta}$ and of certain physical properties of the planet, etc.

Equation (1) is recognized as the equation of a large-angle pendulum, as seen in a frame rotating at a rate $\frac{k}{2}n$ about the pivot axis of the pendulum. We may understand the manner of planet spin capture into a resonance, and the significance of the functional form of T on the probabilities of capture or penetration, by considering the familiar behavior of a large-angle pendulum.

The motion of the pendulum mimics the motion of the planet relative to a uniformly rotating frame having angular velocity $\frac{k}{2}n$. The shaft rotation rate in this analog corresponds to the difference between the planet's resonance rotation rate $\frac{k}{2}n$ and that rotation rate for which the average tidal torque vanishes.

Unfortunately, this pendulum model does little more than illustrate how it is possible that different initial conditions of motion may lead to either resonance capture, or to nonsynchronous rotation at a rate determined by the tidal torque, with varying probabilities dependent on properties of the tidal torque, etc.

In order to obtain answers to the questions we have posed, we intend to apply techniques of analysis that have been developed to study nonlinear systems in the theory of automatic control. Z-transform theory has been found useful to study the properties of the difference equations, derived by Bellomo, Colombo, and Shapiro to describe the state of the planet at successive perihelia. It is hoped that by application of the method of describing functions, some understanding of the nonlinear behavior farther from resonance may be gained. Possibly, known techniques of nonlinear stability theory may be brought to bear.

REFERENCES

1 Bellomo, E., Colombo, G., and Shapiro, I. I., 1966, Symposium on Mantles of the Earth and Terrestrial Planets, Newcastle, England.

2 Colombo, G., 1965, Nature, 208, 575.

3 Colombo, G., and Shapiro, I. I., 1965, Smithsonian Astrophysical Observatory Sp. Rpt., 188 R, 1. See also Colombo, G. and Shapiro, I. I., 1966, Ap. J., 144 (in press).

4 Dyce, R. B., Pettengill, G. H., and Shapiro, I. I., 1966, (to be published).

5 Goldreich, P., 1965, Nature, 208, 375.

6 _____, 1966, Astron. J., 71, 1.

7 Goldreich, P., and Peale, S., 1966a, Nature, 209, 1078.

8 Peale, S., and Gold, T., 1965, Nature, 206, 1240.

9 Pettengill, G., and Dyce, R., 1965, Nature, 206, 1240.

10 Shapiro, I., 1966 (private communication).

11 Goldreich, P., and Peale, S., 1966b, Astron. J., 71, 6.

CHAPTER XV

LOW LEVEL ACCELERATION MEASUREMENT APPARATUS

by

S. Ezekiel

Introduction

The need for low level acceleration (or force) measurement has been evident for some time. The main applications are in the inertial guidance of low-thrust space vehicles, stabilization of test tables for sensitive inertial components, microseismology, and gravity research. At the present time, devices are available for reliable measurement of acceleration down to about 10^{-6} g. Sensitivities approaching 10^{-9} g have been claimed but the calibration and stability of such instruments is open to serious question.

The LLAMA program was an investigation of techniques for the construction of an accelerometer with a threshold sensitivity below 10^{-6} g. A comprehensive report on LLAMA is given in EAL report RE-23.

Basically, the apparatus (Fig. 1) consists of a linear, single-axis accelerometer using a small permanent magnet as a proof mass supported by magnetic forces inside a superconducting cylinder. Coaxial coils on either side of the magnet, inside the cylinder, are used to compensate the slight axial instability of the magnet and also to provide the restoring force to keep the magnet at null. A sensitive displacement detector is employed to feed the restoring coils with control information. Calibration below 10^{-6} g is to be effected by controlled radiation pressure.

Meissner-Effect Suspension

Several types of low-threshold suspensions were considered including feedback stabilized magnetic, electrostatic, charged particle, and cryogenic-magnetic. The final choice was to use the diamagnetism (Meissner Effect) of a superconductor to support a small permanent magnet. A single-axis suspension was constructed by floating the magnet inside a superconducting cylinder so that it was in stable equilibrium radially and slightly unstable axially if displaced from the center of the cylinder. The float height was about one centimeter. Two coils on either side of the magnet (see Fig. 2) compensated for the axial instability. A copper sleeve

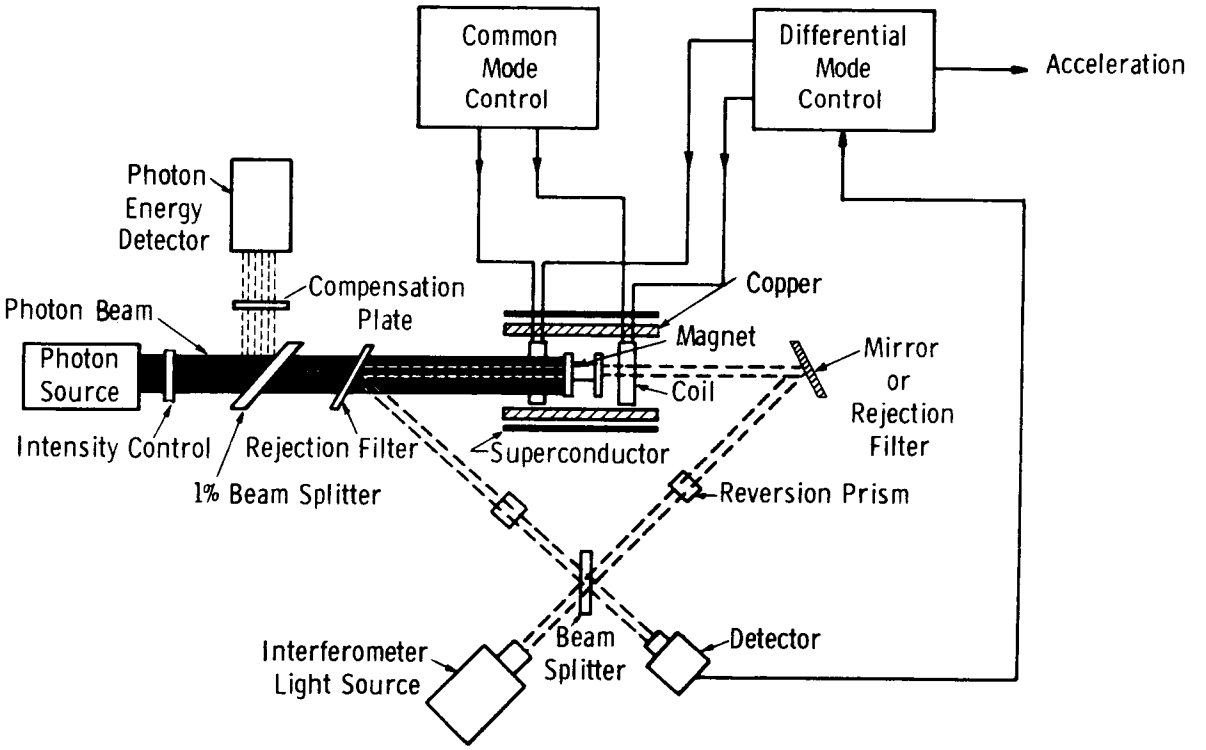

Fig. 1 The LLAMA system.

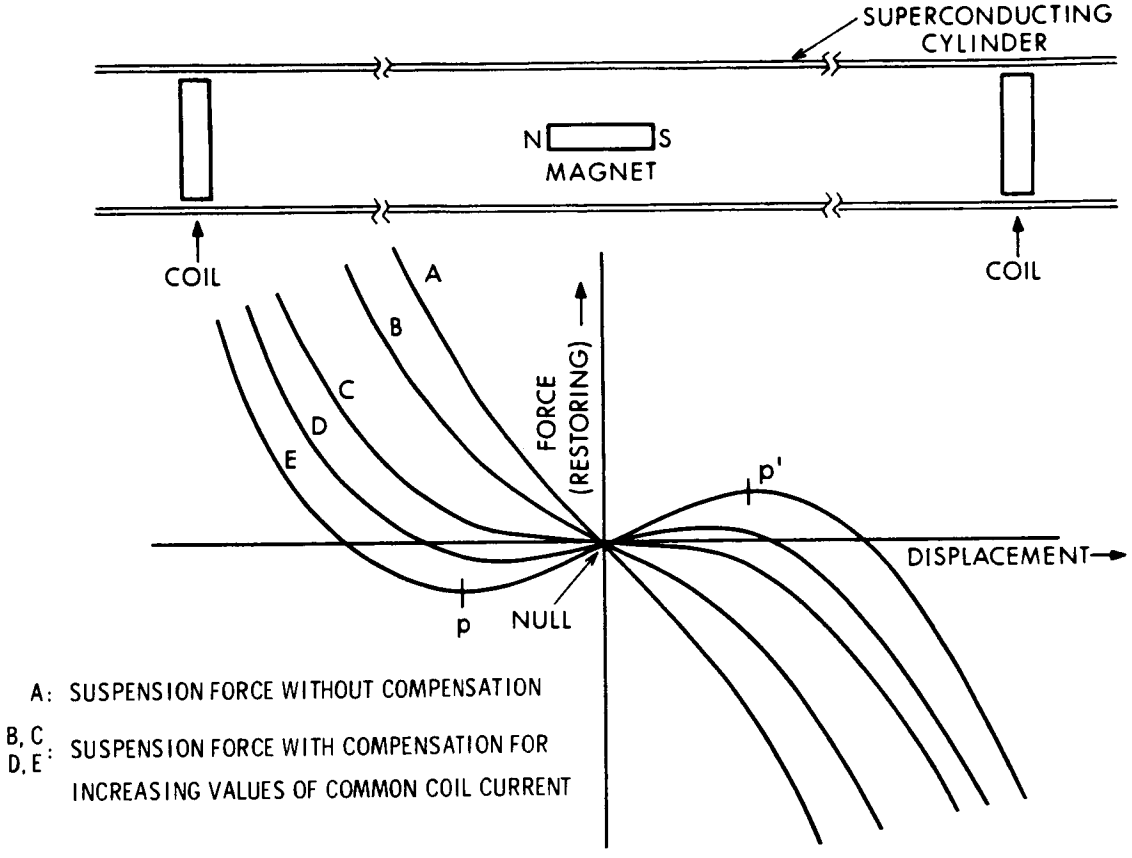

Fig. 2 Axial force on magnet close to null.

within the superconducting cylinder provided some eddy current damping; an axial slit along the top of the cylinder prevented circulating super currents.

Despite the difficulty of operation at cryogenic temperatures, it was considered that this type of suspension offered simplicity of design, long-term dimensional stability, and compatibility with sensitive optical displacement detectors and radiation pressure calibration techniques. Machining tolerance of the cylinder was not as critical as that in an electrostatic suspension because of the greater float height, 1 cm, in the superconducting suspension.

Figure 3 shows a photograph of the magnet floating inside the superconducting cylinder and Fig. 4 shows an early version of the LLAMA dewar.

Displacement Detection

Very small axial displacements, on the order of a fraction of a micron, must be detected in order to preserve an adequate bandwidth at low acceleration levels. For example, at an acceleration of 10^{-6} g, the time taken to move, say, 1 mm is 14 seconds. Other reasons for desiring high sensitivity displacement detection include the tolerance of larger axial suspension spring constants and the reduction in the effects of non-linearity in the suspension and in the detector.

An interferometric scheme using a laser was designed to measure displacements below one micron. Figure 5 shows the layout of this scheme. Two flat mirrors attached to the ends of the magnet constituted the principal mirrors in a differential interferometer. One problem was to make the interferometer insensitive to rotations of the magnet and the other was to keep the magnet sufficiently still so that its position could be held by the interferometer feedback loop.

Insensitivity to transverse rotations was overcome by inverting the image of the magnet in one arm of the interferometer for both transverse axes of rotation of the magnet. This was achieved by placing one dove or inverting prism in each arm of the interferometer with the axes of the prisms at right angles to each other.

Since the interferometer was insensitive to where the quiescent axial position of the magnet was along the tube, a means of holding the magnet in the null region had to be devised before the interferometer could be brought into operation. A less sensitive displacement detector using spot occultation was designed, where displacements of the magnet occulted a beam of light, as shown in Fig. 6. The linear range of this detector was 0.6 mm and the uncertainty range was about ± 2 microns.

Performance of Experimental Accelerometer

A feedback loop was closed around the floating magnet using the spot occultation displacement detector. The damping of the closed loop oscillations is shown in Fig. 7. Threshold sensitivity was below 10^{-6} g and was only limited by the

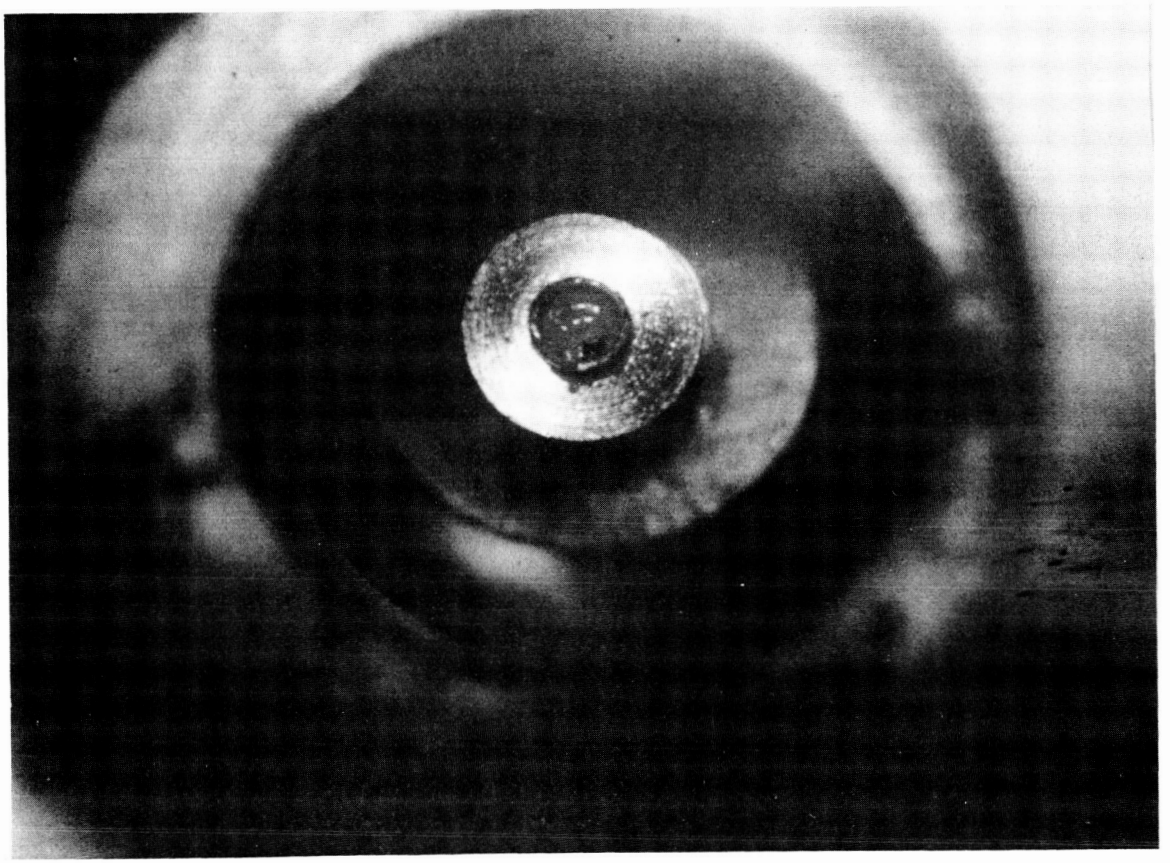

Fig. 3 Magnet floating in LLAMA suspension.

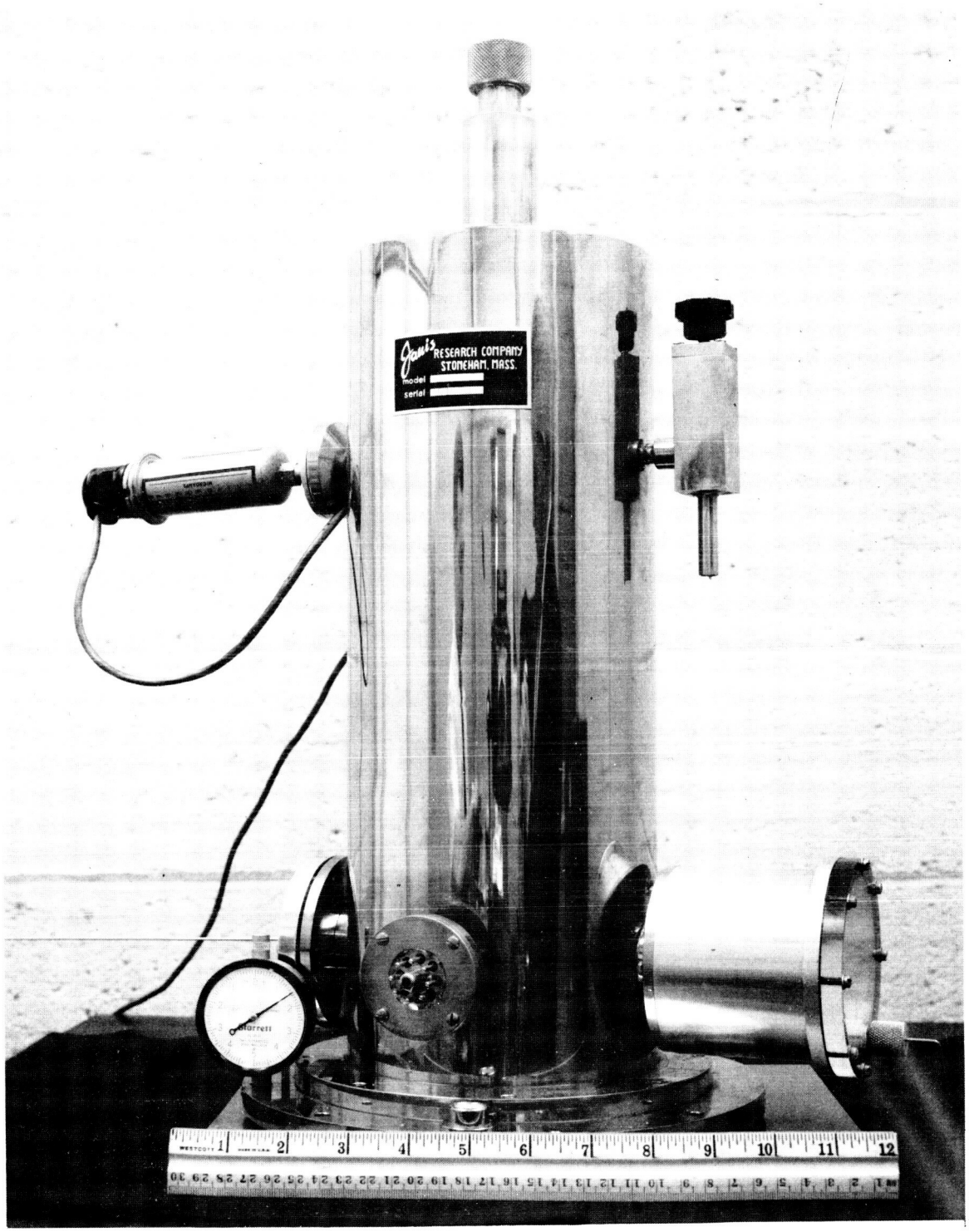

Fig. 4 The LLAMA dewar (early model).

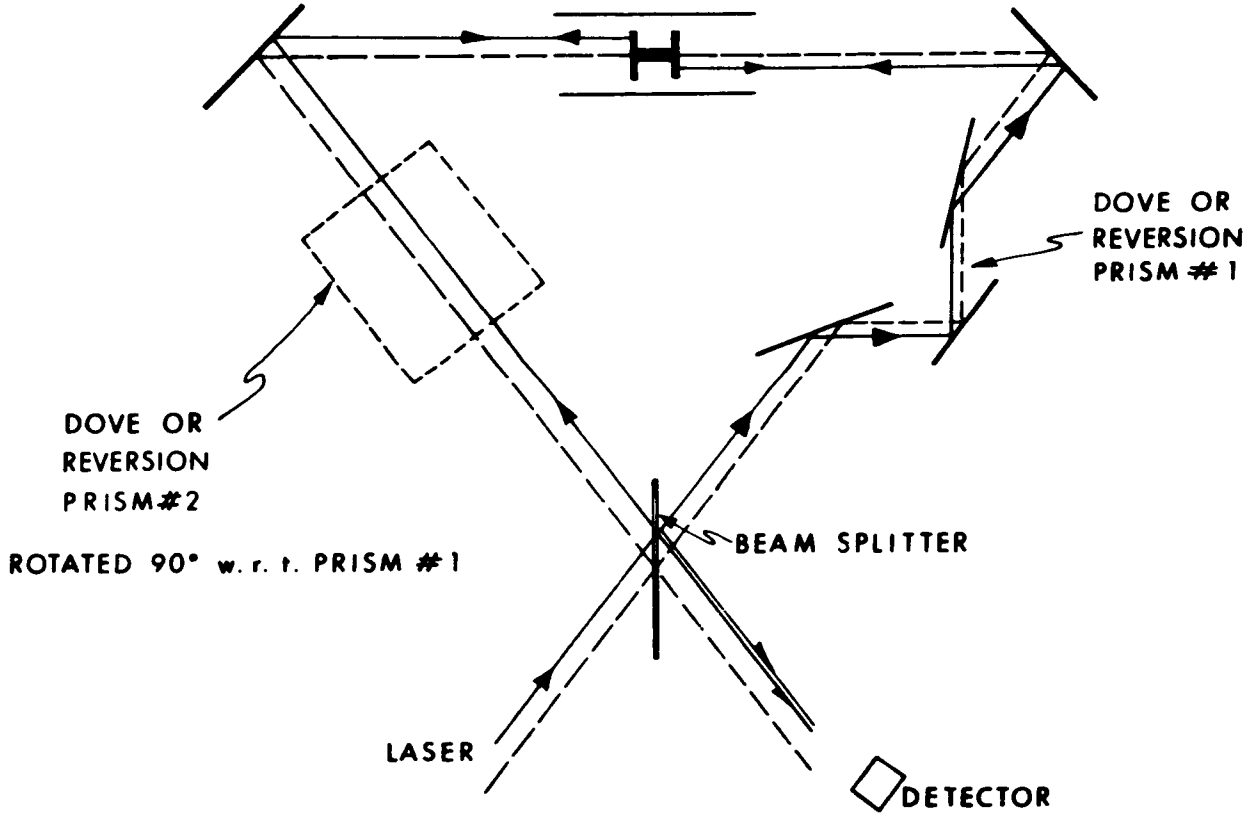

Fig. 5 LLAMA IDD with dove prisms.

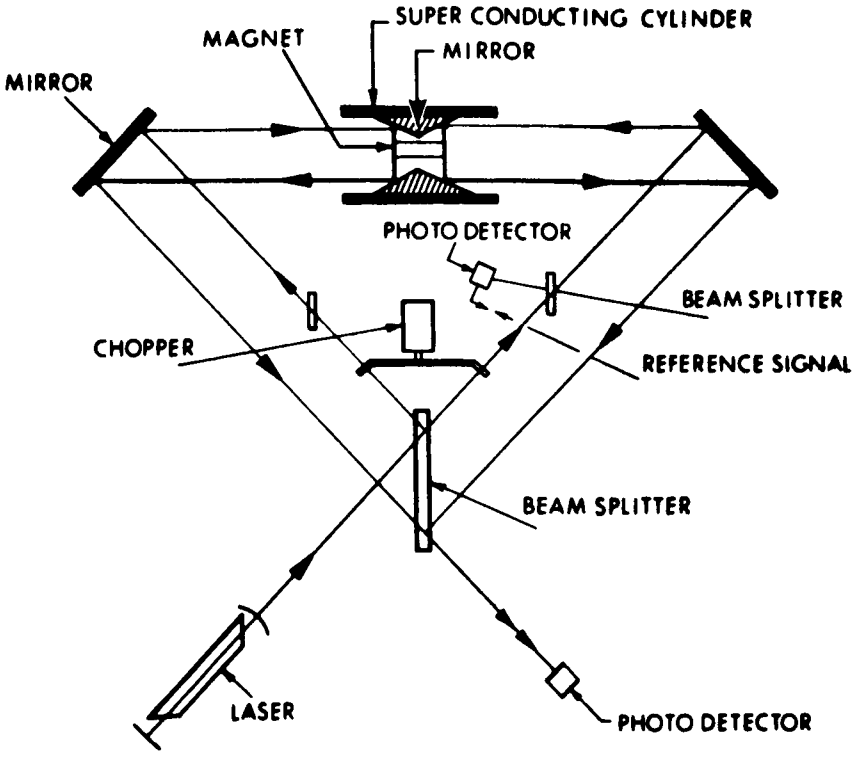

Fig. 6 Spot occulation displacement detector (SODD).

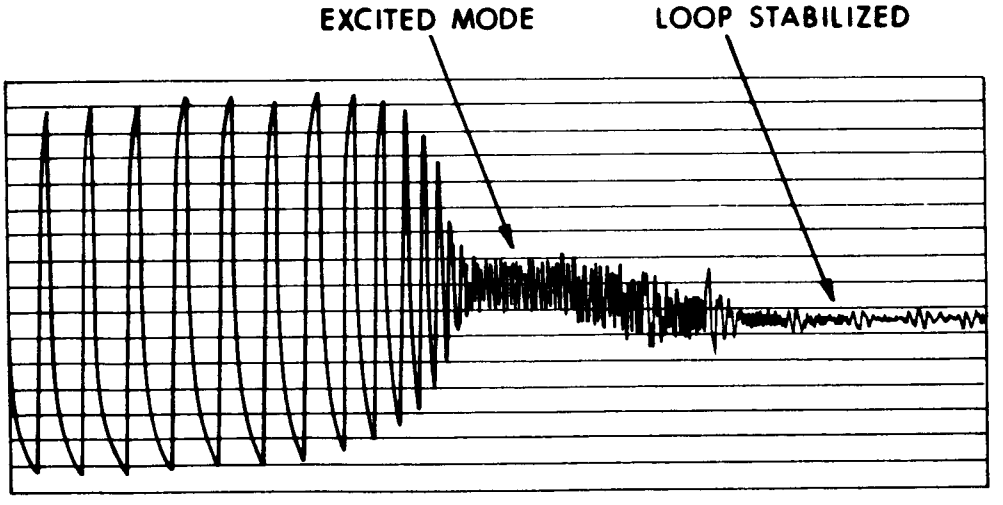

Fig. 7 Damping of closed-loop oscillation.

environment and the displacement detector, rather than by the suspension itself.

When the interferometer displacement detector was used with the floating magnet, several problems came to light which were not present when the suspension simulator was used to verify the interferometric scheme. Because rotation of the magnet about the sensitive axis is very lightly damped, any slight misalignment of the principal mirrors on the magnet prevented the interfering spots from overlapping continuously. Extra care was taken in attaching the mirrors so that they were parallel and as nearly concentric with the magnet as possible to reduce pendulosity effects. Ideally it would be desirable to have the principal mirrors integral with the magnet. Grinding the ends of the magnet flat and parallel is worth exploration. The pendulosity effects that remain would be due to a possible separation of the center of gravity from the magnetic axis of the magnet.

In order to reduce the effect of jittery environment path, length modulation in the interferometer can be introduced. The modulation frequency should be as high as possible so that it is outside the 1/f noise.

Calibration

Accurate calibration of low-level accelerometers has always been difficult if not impossible on the earth. LLAMA offers a distinct advantage in that a means of absolute calibration, within 15%, at these low-levels is feasible.

Since the mass of the magnet is about one gram, an external force of 10^{-3} dynes corresponds to an acceleration of 10^{-6} g. A one-watt beam of light falling normally on a perfectly reflecting surface exerts a force of 0.66×10^{-3} dynes. The only requirements are that there must be a high vacuum environment below 10^{-5} mm Hg, and that the work function of the surface must be higher than the energy of the incident photon to eliminate the generation of photo-electrons. The pressure inside the dewar is better than 10^{-7} mm Hg due to the cryogenic pumping action of the liquid helium and the LLAMA test mass is accessible from outside by means of windows. Lasers can now produce powers in excess of one-watt so that light pressure is well worth exploring. A discussion of radiation pressure calibration is found in RE-23.

Further Work

At present, work on LLAMA is being continued at NASA's Electronics Research Center in Cambridge. Several improvements and suggestions are discussed in RE-23 and it is hoped that further investigations of the LLAMA principles may eventually find the ultimate limitations of such a suspension.

CHAPTER XVI

LONG-TERM LASER FREQUENCY STABILIZATION USING A MOLECULAR BEAM*

by

S. Ezekiel

Need for Long-Term Frequency Stable Lasers

The short-term frequency stability of a free running gas laser, although excellent $\frac{\Delta\nu}{\nu} \approx 10^{-10}$ for a few seconds, is not too suitable for sensitive measurements that require long periods of time. Long-term frequency stability for periods of days, months, years, say, is needed to improve on the present length standard which is one part in 10^8 and to maintain it over long periods. Related to length and optical frequency standards, long-term stability is required:

(a) to enable long-term, long-path interferometric measurements to be made for use in, for example, strain seismometry, and other geophysical measurements such as changes in the radius of the earth and continental drift;

(b) to improve the long-term performance of a laser inertial sensor;

(c) to measure a possible secular variation in the velocity of light; and,

(d) to improve laser communication and laser Doppler navigation.

Sources of Frequency Instability

The main source of frequency drift in a free-running gas laser is the fluctuation of the length of the optical cavity caused by thermal and vibrational effects and by material creep.

The center of the Doppler-broadened gain curve does not coincide with the true resonance frequency of the individual atoms due to pressure shifts and shifts that depend on discharge conditions. The exact frequency of oscillation, therefore, cannot be known to a high degree of precision.

* A joint project with MIT Research Laboratory of Electronics under the direction of Professor R. Weiss of the department of physics.

Present Status of Frequency Stabilization Techniques

Various feedback stabilization techniques have been and are being investigated. Methods of stabilization include:

(a) locking to the Lamb dip at the center of the Doppler-broadened gain curve;

(b) locking the laser frequency to an identical transition in an external discharge cell;

(c) using an external high Ω optical resonator as a frequency discriminator; and,

(d) using a two-beam interferometer as a frequency discriminator.

Scheme (a) suffers from pressure shifts; scheme (b) suffers from pressure shifts as well as Doppler-broadening; and schemes (c) and (d) suffer from temperature dependence and material creep. In none of the above methods can the frequency of the laser be known to better than one part in 10^9.

Ideally, what is required is a primary frequency standard to which the laser frequency can be locked.

Proposed Approach

The proposed approach is to use an atomic (or molecular) beam as the frequency reference for the long term stabilization of a laser.

Atomic beams provide one of the most accurate microwave frequency standards, as in atomic beam clocks whose long-term frequency stability is better than one part in 10^{12}. For this application, then, the standard optical frequency is the absorption line of the extremely stable quantum mechanical oscillator-the isolated atom (or molecule). In contrast with the gas cell, the atoms in an atomic beam may not suffer pressure shift or broadening of their spectral lines because the atoms are kept sufficiently apart to cause the minimum of interaction. Doppler-broadening can be made negligible by arranging the laser beam to be normal to the atomic beam, since the position of both beams is well defined. An atomic beam, then, has an absorption linewidth that is very close to the natural linewidth of the atoms and is centered around the true resonance frequency of the transition.

In order to use an atomic beam for this application several schemes may be investigated.

(a) One method is to find a close match, better than one part in 10^5, between a laser cw line and an optical transition from the ground state or a metastable state (lifetime greater than 10^{-3} seconds) of a suitable atom or molecule.

(b) Another method is to use a 2-photon resonance at the interaction region with the beam atom (or molecule) starting out in either the ground state or a metastable state. The first photon comes from an external light source and the second from the laser. The atom in the beam is identical with the lasing atom.

(c) Another alternative is to design a laser that employs an atom or molecule for which the lower level of the oscillating transition is long-lived in the isolated conditions of the beam but can be made to have a short lifetime in the atmosphere of the laser by means of collision quenching or field quenching.

The resettability of the laser frequency which is important in many applications is only a matter of signal-to-noise, in this case, since a primary frequency reference is used.

Scheme Being Investigated

After a thorough search into atomic and molecular energy levels with the aid of a computer, several close matches have been found between laser lines and ground state and metastable state transitions in atoms and molecules. The scheme under investigation uses the match between an Argon ion laser and a magnetic dipole transition from the ground state of a Rubidium atom.

The experimental set up is shown in Fig. 1. Rubidium atoms in the oven effuse through a narrow slit into a highly evacuated beam chamber. The A- and B-magnets provide inhomogeneous magnetic fields. The A-magnet selects atoms with a given magnetic moment which would terminate on the detector in the absence of the B-magnet. The laser beam interacts with the atomic beam at right angles in the C-region. When the laser frequency coincides with the atomic resonance, the atoms are excited to a higher state from which they decay back to the ground state. As a result, a certain fraction of the atoms will have reversed their magnetic moment due to spin flipping of the outer electron. These atoms will now be deflected into the detector by the B-magnet. The detector signal provides a measure of where the laser frequency is with respect to the atomic resonance. The detector output can therefore be used to tune the laser so as to keep its frequency on the atomic resonance.

A long term frequency stability and resettability better than one part in 10^{10} is anticipated.

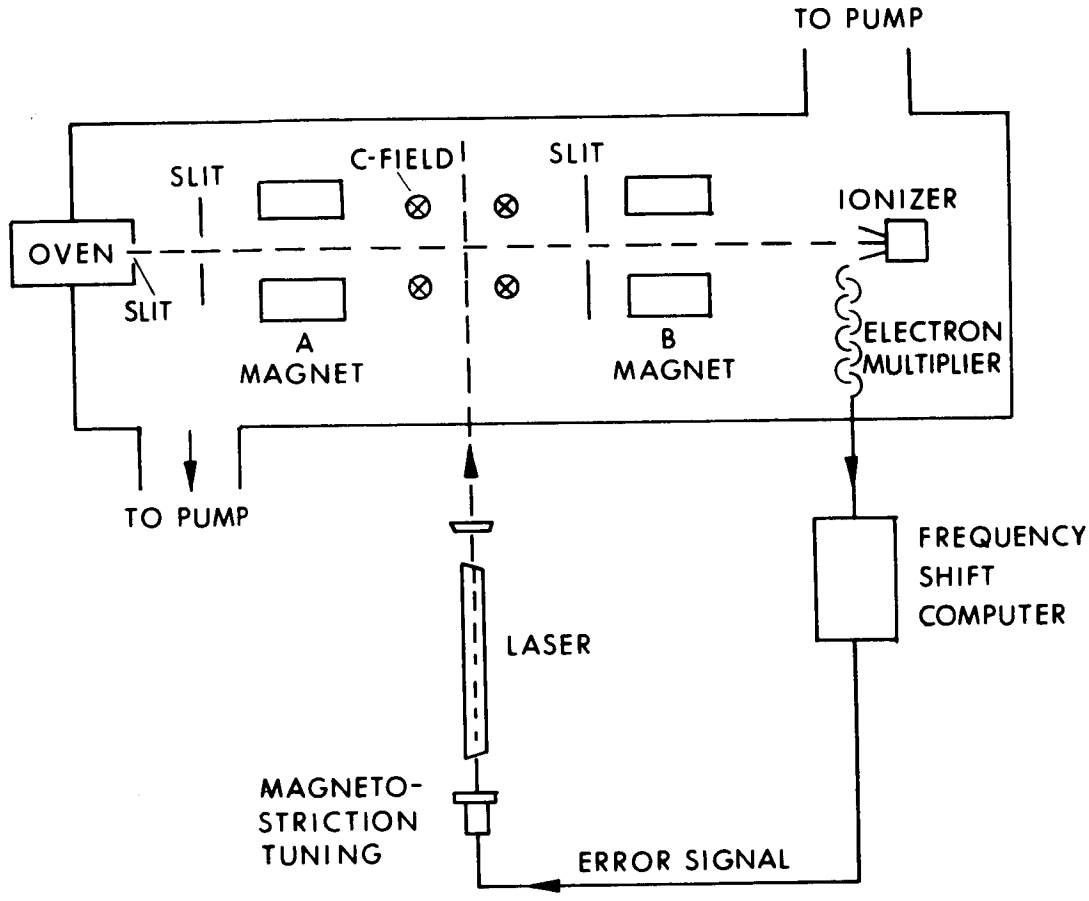

Fig. 1 Scheme being investigated.

CHAPTER XVII

GYRO AND ACCELEROMETER TEST PLATFORM

by

J. T. Egan

The goal of this program with the NASA-Electronic Research Center is to develop a test table to evaluate any accelerometers and gyros which may be developed in the next decade. We are assisting Weinstock of the Electronic Research Center in making a feasibility study and our immediate task is to help him make a working model of a stabilized testing platform. The first test table will have a single-axis leveling system but later will be modified to a two-axis configuration with a horizontal motion isolation device.

Initially, we will attempt to maintain levelness to within 0.01 arc-second and to isolate rotational ground noise up to 25 cycles per second.

To outline the problem let us ignore the rotation of the earth and consider the two general categories of local earth motion. These may be roughly classified as man-made vibrations in the 1 to 10 cycle per second range with amplitudes up to a few mils and rotations up to about 4 arc-seconds, and seismic motions with periods ranging from 1 second to 24 hours with amplitudes of several inches and rotations of about 12 arc-seconds. In practice, and subject to further study, the rotations about a vertical axis and the vertical displacement may be ignored. If these vibrations are not compensated, it will be because the instruments we anticipate testing will be insensitive to these motions.

Others have studied this problem and one solution was to build a very heavy test pad mounted on air bearings to isolate the higher frequency horizontal motions and use low-frequency leveling about two horizontal axes. This type of facility would normally be mounted in a region selected for quiet seismic conditions and freedom from man-made disturbances. In practice, such a location leads to an inconvenient and remote test site.

In contrast, the NASA-Electronic Research Center facility is to achieve vibration isolation through servo control so that, within reasonable limits, a test area may be set up in any convenient room. This program will also isolate against higher frequency disturbances than previous efforts.

The usual sensors for stable platforms are sensitive levels and gyros. The Aerosmith tiltmeter is typical of the sensitive levels. These instruments use two connected mercury pools in which changes in relative mercury surface heights as small as one microinch are sensed by an electronic circuit. The particular model we are using has a nominal accuracy of about 1/60 arc-second and a time response of about 10 seconds. The angular accuracy should improve in a stabilized platform environment. Greater accuracy may also be achieved by placing the mercury pools further apart.

This type of level will define the local direction of gravity which varies with time. The gravity direction will typically oscillate about 12 arc-seconds with a period of about 12 hours.

This class of instrument has two inherent disadvantages in that it is sensitive to horizontal accelerations in any direction and it has long time constants.

For higher frequency sensing, we are using Kearfott inertial gyros, known as the King II gas-bearing gyro. These inertial sensors complement the levels in that they are insensitive to linear accelerations, and are best suited for sensing the higher frequency rotations.

The program is in no way limited to the sensors mentioned but they are typical of the best available of their type.

The Electronic Research Center and Experimental Astronomy Laboratory are now making a single-axis table leveling device which uses two hydraulic pistons in series. One piston is a torque motor,ball bearing screw, hydraulic force amplifier system. This force amplifier is a rugged hydraulic "micromotion drive" developed by the M.I.T. Instrumentation Laboratory. The drive uses a small horizontal input axis bellows working into a hydraulic fluid which will cause a bellows with 25 times the effective area to lift on a vertical axis. The other piston will control the output of a 5 H.P. hydraulic pump feeding into an elevating piston. Both pistons will be required to support 1500 lb and to maintain a height correct to within 3 microinches.

The complex servo design is being carried out by the Electronics Research Center. Frequency and amplitude information of the earth motions in the Cambridge area are not well known and some of this data such as low-frequency displacements are very difficult to measure. Very little earth motion information suitable for our needs has been published. Seismologists are usually interested in local abnormalities in earth motions and the time of their occurance. Their stations are normally located away from industrial areas.

The test requirements suggest that compiling of test data would be tedious unless a pure gravitational direction reference or a pure inertial reference can be maintained. These requirements can be met if the 12 arc-second, 12 hour period (tidal) wandering of the gravity direction plus other low frequency components can be inserted into or removed from the sensor system. For the moment duplicate sensors are being used. The passage within one mercury level may be restricted to increase the time constant to any desired value which makes a very useful averaging device.

After evaluation of the single axis system, we plan to add another horizontal axis and, when available, a two-axis horizontal motion isolator.

From tests and past experience we realize that two-axis sensor leveling and close temperature control are required for optimum sensor performance. We are now mounting all sensors in constant temperature ovens.

It is an accepted requirement in a gyro test facility such as this that the table error sensor performance exceed that of the instruments being tested. This normally leads to early obsolescence, but in this case it is anticipated that as better inertial components are developed improved error sensors will be used.

Page intentionally left blank

APPENDIX A

ATTENDEES OF 5 JANUARY 1967, EAL PROGRAM REVIEW

Analytical Mechanics Associates

T. Edelbaum
A. H. Jazwinski
S. Pines

Bellcomm Corporation

W. G. Heffron
R. V. Sperry

Harvard University

Prof. A. E. Bryson
M. N. Desai
L. Henrikson
R. K. Mehra
J. Turnbull
D. Winfield

ITT Research Institute

A. Friedlander

MIT Experimental Astronomy Laboratory

B. Blood
N. A. Carlson
C. C. Counselman
R. E. Curry
J. Deyst
T. Egan
S. Ezekiel
H. Jones
W. K. Lim
Dr. S. Madden

Experimental Astronomy Laboratory (Continued)

Prof. W. R. Markey
W. J. McDonald
G. Nielson
E. A. Olsson
Prof. J. Potter
C. F. Price
J. Prussing
Dr. R. G. Stern
Prof. W. Wrigley
R. Young

MIT Lincoln Laboratories

Dr. I. I. Shapiro

NASA Electronics Research Center

J. F. Bellantoni
M. Dixon
Dr. R. Hoelker
Dr. G. Kovatch
Dr. R. Langford
Dr. W. L. Lees
Dr. O'Mathuna
W. E. Miner
Dr. M. Payne
D. Rockwell
Dr. F. Tung
H. Weinstock
Miss L. Wilson

NASA Headquarters

J. I. Kanter

NASA Langley Research Center

J. R. Elliott

NASA Manned Spacecraft Center

W. J. Rhine

North American Aviation, Autonetics Division

J. Fagan

U. S. Air Force Academy

Capt. R. E. Willes (USAF)

Yale University

Prof. V. Szebehely

Page intentionally left blank

APPENDIX B

EAL REPORTS AND THESES PUBLISHED UNDER NASA SPONSORSHIP:

RE-3	"Statistical Filtering of Space Navigation Measurements"	Potter, J. E. Stern, R. G. Aug. 1963	a
RE-4	"Analytic Solution of the Equations of Motion of an Interplanetary Space Vehicle in the Midcourse Phase of its Flight"	Stern, R. G. Nov. 1963	a
RE-7	"Selection of Optical Sightings for Position Determination in Interplanetary Space"	Stern, R. G. April 1964	a
RE-8	"Singularities in the Analytic Solution of the Linearized Variational Equations of Elliptical Motion"	Stern, R. G. May 1964	a
RE-9	"A Matrix Equation Arising in Statistical Filter Theory"	Potter, J. E. Feb. 1965	a
RE-11	"A Guidance-Navigation Separation Theorem"	Potter, J. E. Aug. 1964	a
RE-13	"A Sensitive Cryogenic Accelerometer"	Chapman, P. K. Ezekiel, S. Oct. 1964	b
RE-14	"Two-Body Linear Guidance Matrices"	Abrahamson, L. P. Stern, R. G. March 1965 (Rev. June 1965)	a
RE-16	"Optimum Transfer to Mars via Venus"	Hollister, W. M. Prussing, J. E. April 1965	b

RE-17	"Optimization of Midcourse Velocity Corrections"	Stern, R. G. Potter, J. E. Nov. 1965	a
RE-18	"Simplified Midcourse Guidance Techniques"	Slater, G. L. Stern, R. G. Feb. 1966	b
RE-19	"A Special-Purpose Interplanetary Trajectory Computation Program for Guidance and Navigation Studies"	McDonald, W. T. July 1965	a
RE-20	"Linear Many-Body Guidance"	Tanabe, Toru Nov. 1965	a
RE-21	"An Adaptive Gyrocompass System for Attitude Reference on Interplanetary Trajectories"	McDonald, W. T. Dec. 1965	a
RE-23	"Analytical and Experimental Investigations of Low-Level Acceleration Measurement Techniques"	Ezekiel, S. Chapman, P. K. Egan, J. T. April 1966	a
PR-1	"Summary of Experimental Astronomy Laboratory Work on NASA Grant NsG 254-62"	June 1964	c
PR-2	"Summary of Experimental Astronomy Laboratory Work on NASA Grant NsG 264-62"	Blood, B. E. Jan. 1965	c
TE-1	"Spacecraft Attitude Control for Extended Missions" Vol I and II.	New, N. C. May 1963	b
TE-4	"The Mission for a Manned Expedition to Mars"	Hollister, W. M. May 1963	
TE-5	"Interplanetary Midcourse Guidance Analysis" Vol I and II.	Stern, R. G. May 1963	

TE-6	"A High Sensitivity Solid State Light Detector"	Cohen, S. Aug. 1963	
TE-7	"Adaptive Determination of Aircraft Stability Derivatives"	Prussing, J. E. June 1963	
TE-8	"Guidance of Low-Thrust Interplanetary Vehicles"	Mitchell, E. D. June 1964	a
TE-10	"A Cryogenic Test-Mass Suspension for a Sensitive Accelerometer"	Chapman, P. K. June 1964	a
TE-11	"Towards a Low-Level Accelerometer"	Ezekiel, S. June 1964	a
TE-12	"The Correlation of Interplanetary Geometry with Propulsion Requirements for Optimal Low-Thrust Missions"	Carlson, M. Feb. 1965	a
TE-13	"A Statistical Analysis of Gyro Drift Test Data" Vol I	Cooper, J. R. Sept. 1965	a
TE-14	"An Application of the Method of Matched Asymptotic Expansions to Ordinary and Optimal Problems in Hypervelocity Flight Dynamics"	Willes, R. E. Sept. 1966	d
RN-6	"Low-Level Acceleration Measurement Apparatus"	Ezekiel, S. June 1965	c
RN-8	"Special Purpose Space Trajectory Program for Guidance Studies-User's Manual"	McDonald, W. T. July 1965	c
RN-11	"The IPGE System (Interplanetary Guidance System)"	Tanabe, T. Goldberg, A. Dec. 1965	c

Publication Availability Code:

a - available

b - out of print - Xerox copy available upon written request

c - out of print, unavailable

d - in preparation or publication

APPENDIX C

THESES SUPERVISED BY LABORATORY PERSONNEL BUT NOT PUBLISHED AS LABORATORY DOCUMENTS

1. Gielow, R. L., "An Evaluation of the Two-body Non-linear Interplanetary Guidance Technique", M. S., June 1964.
2. Holbrow, W. F., Jr., "Simplified Selection of Optical Fix Data and a Simplified Guidance Technique", M. S., June 1964.
3. Munnell, T. C., "An Analysis of the Application of Two-body Linear Guidance to Space Flights", M. S., September 1964.
4. Love, W. C., "An Investigation of the Capabilites of the Phantom Target Technique in Variable Time-of-Arrival Guidance", M. S., May 1965.
5. Fagan, J. H., and Whitlow, D. W., "Timing Schedule Optimization for Earth Orbit", M. S., June 1965.
6. Ruth, J. C., "Analysis of an Interplanetary Line-of-Sight Guidance Technique", M. S., June 1965.
7. Lim, W. K., "Explicit Non-linear Two-body Guidance Analysis", M. S., January 1966.
8. Eck, J. C., "Simplified Guidance Techniques for Interplanetary Missions", M. S., May 1966.
9. Madl, D. O., "Sunblazer State Determination Investigation", M. S., May 1966.
10. Winston, B. P., "Optimal Four-Impulse Transfer between Two Nearby Orbits", M. S., May 1966.
11. Dierstein, R., "Contributions to the Applicability of Variable Time-of Arrival Guidance for Interplanetary Flight", M. S., June 1966.
12. Doerer, H. T. and Langley, R. W., "Processing Solar Probe Tracking Data", M. S., August 1966.